Seasonal dynamics of methanotrophic bacteria in a boreal oil sands end-pit lake

Emad A. Albakistani[1], Felix C. Nwosu[1], Chantel Furgason[1], Evan S. Haupt[1], Angela V. Smirnova[1], Tobin J. Verbeke[1], Eun-Suk Lee[1], Joong-Jae Kim[1], Amelia Chan[1], Ilona A. Ruhl[1,3], Andriy Sheremet[1], Sarah B. Rudderham[2], Matthew B. J. Lindsay[2], and Peter F. Dunfield*[1]

[1] Department of Biological Sciences, University of Calgary, 2500 University Dr. NW, Calgary, AB, Canada

[2] Department of Geological Sciences, University of Saskatchewan, 114 Science Place, Saskatoon, SK, Canada

[3] National Bioenergy Center, National Renewable Energy Laboratory, Golden, CO, USA

These authors contributed equally to this work: Emad A. Albakistani, Felix Nwosu, Chantel Furgason

*Corresponding author: Peter F. Dunfield, Department of Biological Sciences, University of Calgary, 2500 University Dr. NW Calgary AB Canada T2N 1N4, pfdunfie@ucalgary.ca

Running title: Methanotroph dynamics in a boreal lake

Keywords: methane, methanotroph, stratified lake, dimictic lake, land reclamation

Supplementary File 1: Supplementary Tables

Supplementary File 2: Supplementary Figures

Abstract

Base Mine Lake (BML) is the first full-scale demonstration end pit lake for the oil sands mining industry in Canada. We examined aerobic methanotrophic bacteria over all seasons for five years in this dimictic lake. Methanotrophs comprised up to 58% of all bacterial reads in 16S rRNA gene amplicon sequencing analyses (median 2.8%), and up to 2.7×10^4 cells mL^{-1} of water (median 0.5×10^3) based on qPCR of *pmoA* genes. Methanotrophic activity and populations in the lake water were highest during fall turnover, and remained high through the winter ice-covered period into spring turnover. They declined during summer stratification, especially in the epilimnion. Three methanotroph genera (*Methylobacter*, *Methylovulum*, and *Methyloparacoccus*) cycled seasonally, based on both relative and absolute abundance measurements. *Methylobacter* and *Methylovulum* populations peaked in winter/spring, when methane oxidation activity was psychrophilic. *Methyloparacoccus* populations increased in the water column through summer and fall, when methane oxidation was mesophilic, and also predominated in the underlying tailings sediment. Other, less abundant genera grew primarily during summer, possibly due to distinct CH_4/O_2 microniches created during thermal stratification. These data are consistent with temporal and spatial niche differentiation based on temperature, CH_4 and O_2. This pit lake displays methane cycling and methanotroph population dynamics similar to natural boreal lakes.

Importance statement:

The study examined methanotrophic bacteria in an industrial end pit lake, combining molecular DNA methods (both quantitative and descriptive) with biogeochemical measurements. The lake was sampled over 5 years, in all four seasons, as often as weekly, and included sub-ice samples.

The resulting multi-season and multi-year dataset is unique in its size and intensity, and allowed us to document clear and consistent seasonal patterns of growth and decline of three methanotroph genera (*Methylobacter*, *Methylovulum*, and *Methyloparacoccus*). Laboratory experiments suggested that one major control of this succession was niche partitioning based on temperature. The study helps to understand microbial dynamics in engineered end-pit lakes, but we propose that the dynamics are typical of boreal stratified lakes, and widely applicable in microbial ecology and limnology. Methane oxidising bacteria are important model organisms in microbial ecology, and have implications for global climate change.

Introduction

Oil sand is a matrix of inorganic particles, water, and bitumen. Extraction of marketable oil from surface oil sands deposits in Alberta, Canada is achieved via treatment with hot caustic water and naphtha/paraffin solvents. This process produces fluid fine tailings (FFT) comprised of alkaline water (pH =10), silt, clay, residual bitumen, salts, and unrecovered solvents (1-4). FFT are stored in open tailings ponds, from which water is recycled to the extraction plant. However, mine operators are ultimately required to reclaim mined lands to an "equivalent land capability" of the original landscape (5). Wet landscape approaches to reclamation involve the creation of engineered bogs, fens, or end pit lakes (EPLs) in which FFT are contained and remediated over time (3). EPLs, below-grade bodies of water constructed in surface mining pits, are common in other sectors of the mining industry. However, proposed oil sands EPLs are shallower and larger in area than most EPLs, and their environmental issues arise from organic pollutants and dissolved salts rather than acidification and metal toxicity (6). Only one full-scale demonstration EPL presently exists in the Alberta oil sands region: Base Mine Lake (BML). BML is an approximately 780-ha lake created from an exhausted mining pit filled with about 45-m-depth of FFT and capped with fresh water in 2012 (2). The water cap at the time of the present study was 10-12 m deep (7). There is a clear boundary between the sedimented tailings material (called sediment in this text) and the water cap. BML behaves as a typical boreal dimictic lake with summer and winter stratification periods separated by spring and fall turnover events (8, 9).

Solvents used in bitumen extraction, and to a lesser extent bitumen itself, are substrates for methanogenesis (10-12). Active oil sands tailings ponds can therefore be strongly methanogenic, emitting 30-26,000 kg CH_4 ha^{-1} annually (13). Although tailings are no longer being deposited

into BML, methanogenesis of the deposited solvents has continued. Methane emissions from BML averaged 610 kg ha^{-1} y^{-1} between 2014-2019, with a gradual decline over time (14). Emissions are highest during spring thaw, when methane that accumulates under the ice cover is released (14). Dissolved methane concentrations in the sediment are very high, and increase rapidly with depth. In 2016 and 2017, concentrations ranged from < 0.1 mM at the sediment-water interface to > 2 mM at a depth of 1.0 - 1.5 m in the FFT layer (15), and reached saturation (~4 mM) at 1.5-3.5 m depth in the FFT (16). During summer stratification, a methane gradient is also evident in the water column, ranging from 20–40 μM in the hypolimnion (subsurface zone, 6-9 m) to 0.38-1.2 μM in the epilimnion (surface zone, 0-4 m) (7). Dissolved O_2 is present throughout the water column, from 70-85% of saturation at the top of the metalimnion (4-6 m) to 1-5% saturation at the sediment interface (7). The hypolimnion remains somewhat oxic due to physical mixing processes from the epilimnion (16, 17). These methane/O_2 counter gradients indicate that active aerobic methane oxidation occurs in the metalimnion, hypolimnion and sediment-water interface of BML. In fact, O_2 consumption in the lake was shown in 2016 to be largely driven by methane and NH_4^+ oxidation (7).

Although methanogenic substrates in natural lakes are primarily plant or algal polysaccharides rather than petroleum hydrocarbons, an active methane cycle is common in temperate and boreal lakes, which are major sources of atmospheric methane globally (18). In seasonally ice-covered lakes methane is emitted via diffusive and ebullitive fluxes as well as an episodic spring thaw flux that accounts for an average of 27% of total annual emissions (19, 20). However, much of the methane produced in natural lakes (30%-99%) is not emitted to the atmosphere, but rather oxidised by aerobic methanotrophic bacteria in oxic water or sediment layers (21, 22). Aerobic

methanotrophs comprise a few taxonomic clusters of bacteria that use methane monooxygenase (MMO) enzymes to oxidise methane to methanol, which is then metabolised for energy and carbon. In temperate and boreal areas, *Alphaproteobacteria* methanotrophs (families *Methylocystaceae* and *Beijerinckiaceae*) predominate under acidic and oligotrophic conditions, such as in *Sphagnum* bogs and bog-lakes, while *Gammaproteobacteria* methanotrophs (family *Methylococcaceae*) are predominant in pH-neutral minerotrophic environments, including most lake waters and sediments (23, 24). Typical gammaproteobacterial genera found in seasonally stratified lakes include *Methylobacter*, *Methyloparacoccus, Methylomonas, Methylosoma,* and *Crenothrix* (24-28). Methanotrophs are usually present throughout the water column but their activity may peak in the oxycline, which is located in the metalimnion when the hypolimnion is anoxic (e.g. in eutrophic lakes (29-31), or at the sediment interface when the hypolimnion is oxic (32, 33). Methane oxidation rates can peak during fall turnover, when methane stored in the hypolimnion mixes with well-oxygenated surface water (21, 29, 34, 35). Methanotrophic species assemblages in these lakes may change with depth and season (27, 28, 35).

We have previously documented the activity of *Methylococcaceae* methanotrophs in the surface layers of active oil sands tailings ponds (36). In the present study we examined the dynamics of methanotrophic bacteria in a reclaimed end-pit lake, BML. Qualitative and quantitative methods were used to determine community compositions and populations sizes, and assess how these changed with season and depth.

Methods

Sampling

A map of BML (56.7267° N, 111.3790° W) showing the positions of three fixed sampling platforms is provided in Supplementary Fig. 1. A detailed description of BML has been provided in previous studies (2, 9). Briefly, the original mining pit located on this site (West-In Pit, WIP) was begun in 1978 and converted into a tailings pond in 1994. From 1994-2012 it was gradually filled with FFT to a depth of 45-50 m, and in 2012 capped with an additional 5 m of fresh water, forming the present end pit lake, renamed Base Mine Lake. There is no outflow from BML to the local watershed, but the water level is maintained at 308.7 metres above sea level via pump-in of freshwater or pump-out of excess water to the extraction plant (2). Due to gradual FFT settling and dewatering, the depth of the water cap increased to approximately 10-12 m by 2019. BML is dimictic, with ice-on in November, ice-off in April to May, onset of summer stratification in May to June, and fall turnover in September (9). Water temperatures vary from 0-24^{o}C depending on season, and the maximum summer thermal gradient spans about 12^{o}C (8, 9). A schematic describing the seasonal lake dynamics is shown in Supplementary Fig. 2.

Water quality in BML has gradually improved over time. Concentrations of heavy metal and most hydrocarbon contaminants are similar to undisturbed freshwater sites in the region (37). The primary organic contaminants in BML, a class of carboxylic acid extractable compounds known as naphthenic acids, have concentrations near 30 mg L^{-1} (37), whereas freshwater sources in the area contain 1-2 mg L^{-1} (38). The pH of FFT is alkaline (pH = 10), but the FFT porewater has been diluted by freshwater inputs, and the BML water cap has ranged from pH 7.8- 8.6 (37). Due to clay suspension from FFT, water turbidity from 2012-2016 (50-350 NTU) was about an order of magnitude higher than that of freshwater bodies in the region (9). In an attempt to manage the turbidity, a chemical coagulant (aluminum potassium sulfate or alum) was added to

BML in September, 2016 to a final concentration of 1.12 mg of aluminum per L of BML water (37). Turbidity decreased following the alum addition: in 2015, mean turbidity in the water column (0-8 m) ranged from 35-130 NTU and from 2017-2019 it ranged from 2.6-48 NTU (37). Although aluminum inhibits atmospheric methane oxidation in forest soils at concentrations as low as 0.63 μg/g soil (39, 40), high methane oxidation rates in BML (see Results) suggest that there was no adverse effect of alum on methane oxidation. Unfortunately because of the scarcity of pre-alum samples, firm conclusions about the effect of alum addition cannot be made.

At 1-4 week intervals from 2015-2019, 500-mL water samples were taken using Van Dorn water samplers from the surface (0-50 cm) and from c. 1 m above the sediment (tailings) interface, from each of the three fixed sampling platforms in BML (Supplementary Fig. 1). Once every month, samples were also taken from 1-m intervals through the entire water column. Below-ice winter samples were taken after ice-coring. The only major interruption in the sampling program was due to a wildfire in early 2016. A fixed interval sampler was also deployed irregularly to collect samples at 10-cm intervals for 1 m across the sediment-water interface (41). All samples were stored in polypropylene bottles and shipped on ice to the University of Calgary (c. 2 d shipping time). On arrival, samples were stored at 5-8°C, generally for 1-2 d until processing.

Biogeochemical rate measurements

For samples taken in 2015-2017, 5-d Biological Oxygen Demand (BOD5) was estimated. 400 mL of each sample (3 platforms × 2-10 depths on each date) were shaken in 1-L serum bottles at 120 rpm for 15 min to equilibrate with ambient O_2. Dissolved oxygen (DO) was then measured on an Orion Star A323 Dissolved Oxygen/Portable Meter (Thermo Scientific, Waltham, MA,

171 USA) or a Hach HQ440 Portable LDO Meter (Hach, London, Ont. Canada) using a DO probe.
172 Each sample was then filled to the brim of a 100-mL Pyrex bottle and capped with a butyl rubber
173 stopper pierced by two needles that allowed excess sample and air bubbles to be removed during
174 capping. Bottles were incubated for 5 days at 22^{o}C, then DO again measured. BOD5 values were
175 calculated from the loss between 0 and 5 d.
176
177 For each sample, a second BOD5 incubation was performed with methane added to the water to
178 estimate the potential methane oxidation rate. The procedure was exactly as described for BOD,
179 except that in the initial step 10% v/v methane was added to the headspaces of the 1-L serum
180 bottles to equilibrate the water with elevated CH_4 as well as O_2. Subtracting the BOD5 from the
181 BOD5+CH_4 value gave the estimated O_2 demand by methanotrophs, and also the potential
182 methane consumption rate using a stoichiometry of $2O_2$:$1CH_4$. Direct measurement of methane
183 depletion resulted in similar methane oxidation rates as this O_2-based method (see "Temperature
184 response" section).
185
186 **Molecular community analyses via 16S rRNA gene amplicon sequencing**
187 Samples were centrifuged and processed as described in Supplementary Table 1. The pellet of
188 clays + cells was resuspended in about 0.5 mL of sample water, transferred into 2-mL tubes, and
189 frozen at -80°C. DNA was extracted using the FastDNA Extraction Kit for Soil (MP
190 Biomedicals, Santa Ana, CA, USA) with an additional purification step using 5.5 M guanidine
191 thiocyanate (42), and eluted in Qiagen Elution Buffer (Qiagen, Toronto, ON, Canada). DNA
192 extracts quantified with a Qubit HS kit (Invitrogen, Carlsbad, CA, USA) ranged from 5-100 ng
193 μL^{-1}. The V3-V4 region of the 16S rRNA gene was amplified using universal bacterial primers

341fw (5'-CCTACGGGNGGCWGCAG-3') and 785r (5'-GACTACHVGGGTATCTAATCC-3') (43). Amplicons for barcoded Illumina MiSeq analyses were produced as described in (44) using a MiSeq Reagent Kit v3 with 600 cycles (Illumina part number MS-102-3003). A maximum of 400 amplicon samples were sequenced per MiSeq lane, and a total 759 samples and 10,313,858 reads were processed.

Sequence data were analyzed using Quantitative Insights Into Microbial Ecology version 2 (QIIME2) (45). Primers and adaptor sequences were trimmed from all fastq files using cutadapt software (46), and DADA2 was applied to denoise, pair reads, and remove chimerae (47). A quality score was analyzed for 10 random samples per run to adjust denoising parameters. Reads were truncated at position 230 (forward reads) or 210 (reverse reads) from the 3'-end, and at position 20 from the 5'-end. Feature tables from various lanes were merged into a single amplicon sequence variant (ASV) feature table. Taxonomy was assigned using SILVA132 (48). All ASVs attributed to *Eukarya* (504,950 reads and 2,124 ASVs) were removed, leaving a total of 54,848 ASVs. Of these, 29 ASVs were classified to taxonomic genera or families known to contain only methanotrophs (Supplementary Table 2). These 29 ASVs were used in most downstream analyses (GenBank accession numbers: OK217110 - OK217124).

Phylogenetic construction

Phylogenetic constructions were performed using the ARB software (49). Sequences from 16S rRNA gene amplicon analysis were aligned using the ACT aligner of the SILVA website (https://www.arb-silva.de/aligner/) and added to the SILVA 138 SSU reference database (48).

Some SILVA-based assignments of methanotrophic genera were corrected after phylogenetic construction.

For phylogenetic construction based on the methanotroph-specific *pmoA* gene, a custom reference database was used (50), and *pmoA* genes from BML added to this. The *pmoA* genes from BML were obtained from exploratory metagenomes sequenced and assembled as described in Supplementary Table 3. BML metagenomes were queried for *pmoA* genes via HMMER searches (HMMER 3.3.2, http://hmmer.org/) on Prodigal gene prediction software.

pmoA-gene based quantitative PCR

All aerobic methanotrophic genera detected in the 16S rRNA gene amplicon analyses are known to encode a particulate methane monooxygenase (pMMO). *Alphaproteobacteria* genera like *Methyloferula* and *Methylocella* (51) that use only a soluble methane monooxygenase (sMMO) enzyme for methane oxidation were found in only small numbers in BML (<0.5% for 99% of samples based on 16S rRNA relative abundance data). This suggests that methanotrophs in BML can be effectively quantified by targeting the *pmoA* gene, which encodes a subunit of pMMO. qPCR quantification of this gene has been extensively used to identify and quantify methanotrophs in diverse environments (52).

First, three qPCR assays designed by Kolb *et al.* (53) were chosen to target the major genera found in our amplicon analysis. These targeted: i) total proteobacterial methanotrophs (A189/Mb661); ii) *Methylobacter/Methylovulum/Methyloprofundus/Methylosoma* (A189/Mb601); and iii) *Methylococcus/Methyloparacoccus/Methylocaldum* (A189/Mc468), as

shown in Supplementary Table 4. To verify that these primers designed in 2003 were still specific, they were compared to a *pmoA* database assembled from all methanotroph genomes available to 2019 (50), and to the *pmoA* genes retrieved from the BML metagenomes. This proved that the primers designed by (53) were effective, with only one minor modification needed in one primer targeting the *Methylobacter* group (Supplementary Table 4). qPCR was performed in reactions containing 1 µL of sample gDNA, 5.0 µL of SYBR GreenPCR Mix (QIAGEN, Velno, Netherlands), 1.25 µM of each forward/reverse primer, and DNAse-free water to make up to 10-µL (QIAGEN, Velno, Netherlands), on a Rotor-Gene 6000 (QIAGEN, Velno, Netherlands). Standards are described in Supplementary Table 4.

Temperature response

To estimate the temperature response of methane oxidation, 75-mL aliquots of water from winter (March 12-14, 2018) and summer (August 26, 2019) were added to sterile 120-mL serum bottles. Bottles were capped with butyl rubber stoppers, supplemented with 10% (v/v) of CH_4, vigorously shaken to equilibrate the liquid with methane, and filled to the brim with more sample water, taking care to avoid air bubbles. The bottles were incubated at 0, 4, 8, 10, 15, 22, and 30°C. Sterile water was used as a control. After 24 h, 3 mL of water was removed from each bottle with a syringe and injected into an 11-mL capped serum bottle for estimation of dissolved CH_4. Vials were well-shaken and headspace CH_4 determined via gas chromatography on a Model 8610C GC (SRI Instruments, Torrance, CA, USA) equipped with a flame ionization detector (Column 190°C, detector 300°C, and N_2 as carrier gas) and a 0.1-mL sampling loop. The sampled 3-mL of water was replaced. Measurements were carried out at 2- or 3-d intervals until the methane was exhausted (14-33 d). Calculated methane oxidation rates were based on

linear regression of initial, linear rates (generally 24 d). At the end of the incubation, the water was centrifuged at 8,000 g for 10 min and the pellet was used to isolate and process DNA as described above.

Results:

Potential methane oxidation rates

Methane oxidation rates estimated via an O_2 depletion assay were similar to rates estimated via CH_4 depletion, verifying the method. Potential methane oxidation rates in the water column from 2015-2017 are presented in Fig. 1 and Table 1. Winter samples were extremely variable, but a consistent seasonal pattern for the rest of the year was observed. Methane oxidation rates were high during spring and fall. Rates declined during summer stratification, but only in the epilimnion. This effect was significant: methane oxidation rates in summer were significantly higher in the hypolimnion (1 m from the sediment) than in the epilimnion (0.5 m from the surface), based on a paired-sample ANOVA with Bonferroni correction for 2 comparisons ($P=0.014$), but no significant depth or seasonal patterns were detected when the lake was unstratified (Table 1). Examination of samples taken at 1-m intervals verified that methane oxidation rates were similar throughout the water column in fall, winter and spring, but increased with depth during summer stratification (Supplementary Fig. 3).

Seasonal dynamics of methanotrophic bacteria in the water column

Putative methanotrophs made up a large portion of the bacterial community in the water, averaging 9.0% of 16S rRNA (median 2.8%) gene reads in all samples but reaching as high as 58.5% in particular samples. Most (>99%) of the identifiable methanotroph reads belonged to the

Methylococcaceae family of the class *Gammaproteobacteria.* Methanotroph ASVs present in at least 20 samples and with an average relative abundance >0.1% are listed in Supplementary Table 2, and Fig. 2 shows their respective phylogenetic positions. The most abundant ASVs belonged to the genera *Methylobacter, Methyloparacoccus,* and *Methylovulum/Methylosoma* (closely related to both genera, but hereinafter referred to only as *Methylovulum*). Less abundant ASVs were related to the genera *Methyloprofundus, Methylococcus, Crenothrix,* and a few other *Methylococcaceae* that could not be classified to the genus level. *Methylocella* and *Methylocystis* were the most abundant alphaproteobacterial methanotrophs, but comprised only 0.012% and 0.0058%, respectively, of all reads. ASVs belonging to the family *Methylomirabilaceae* were not detected in any BML sample, although they were sometimes detected in a neighboring freshwater reservoir (data not shown).

There was a U-shape in the relative abundance of methanotrophs in 16S rRNA gene amplicon sequencing sets from 2017 to 2019, with the highest relative abundances observed during fall and winter, and the lowest during summer stratification (Fig. 3). This pattern was evident in both surface and bottom waters, although summer abundances in the hypolimnion were higher than in the epilimnion (Supplementary Fig. 4). There was also a regular seasonal succession of the three main genera, evident qualitatively in time courses of ASVs pooled into genus-level groups (Fig. 3), and quantitatively in an Analysis of Composition of Microbiomes (ANCOM) (59) (Fig. 4). *Methyloparacoccus* predominated during late summer and fall turnover, increasing dramatically as fall turnover progressed, while *Methylobacter* and *Methylovulum* dominated in winter and spring, usually declining as summer progressed (Fig. 3, 4). The *Methyloparacoccus* was predominantly (>95%) a single ASV. There were several *Methylovulum* ASVs. Sometimes

different ASVs of this genus predominated in different years, but all showed a similar pattern of peaking in winter/spring (Fig. 4; Supplementary Fig. 5). *Methylobacter* ASVs were more variable: the two most abundant *Methylobacter* ASVs (ASV4 and ASV8) peaked in winter, but others peaked in both winter and mid-summer (Fig. 4; Supplementary Fig. 5). Several less abundant ASVs, including a *Methylococcus* and *Methyloprofundus,* were evident primarily in summer and fall (Fig. 4). The overall alpha diversity of methanotrophs usually peaked in summer (Supplementary Fig. 6), perhaps because summer stratification increased the number of microniches selecting for particular species. A gradual but significant increase in methanotroph diversity was also observed over the 5-year course of the study (Supplementary Fig. 6).

Analyses of *pmoA* genes reinforced the conclusions of 16S rRNA gene sequencing. Complete *pmoA* genes from *Methyloparacoccus* and *Methylobacter* were recovered from metagenomes (Supplementary Fig. 7), supporting the predominance of these genera. The seasonal patterns in *pmoA* gene counts via qPCR closely mirrored the patterns of relative 16S rRNA gene abundances described above. The lowest counts in the universal *pmoA* gene assay were measured in mid-summer (in both the epilimnion and the hypolimnion), and the highest counts in fall and winter (Fig. 5). The *Methylococcus*-group-specific *pmoA* assay (encompassing primarily *Methyloparacoccus* in BML) showed a similar pattern, with the lowest counts in early summer, gradually increasing in late summer and peaking in late fall or early winter (Fig. 5). *Methylobacter*-group-specific *pmoA* counts (encompassing primarily *Methylobacter* and *Methylovulum* ASVs) were highest in winter and spring, then declined gradually throughout the calendar year (Fig. 5). All three patterns match the amplicon-based analyses (Fig. 3-4).

Methylotrophic bacteria in the order *Methylophilales* are known to grow in concert with methanotrophs in oilsands tailings ponds (36). These were also abundant in the water, particularly in winter and spring (Supplementary Fig. 8).

Patterns of methanotrophic bacteria with depth

Similar to the pattern noted for methane oxidation rates, higher methanotroph relative abundances were measured in the hypolimnion than in the epilimnion during summer stratification of each year (Supplementary Fig. 4). In all three *pmoA* qPCR assays, summer hypolimnetic waters also generally had higher *pmoA* gene counts than epilimnetic waters (Fig. 5).

Counts of *pmoA* genes in the surface tailings sediment (to 50-cm depth below the sediment interface) were compared to counts throughout the water column on 4 dates. In each case, regardless of season, 2-4 orders of magnitude higher gene copies were evident in the sediment (Supplementary Fig. 9). Copy numbers of *pmoA* gene in the sediment were consistently high, so probably the methanotrophs in sediment respond to shifting conditions by altering their activity rather than via growth. Based on relative abundances from 16S rRNA gene amplicon sequencing, a zonation of methanotroph genera was observed across the sediment-water interface, with *Methylobacter* dominating just above the sediment interface and *Methyloparacoccus* just below it (Fig. 6). The water column above the sediment interface showed little vertical zonation of the methanotroph genera, but instead displayed the seasonal pattern of *Methyloparacoccus* predominating in summer and fall, and *Methylobacter* and *Methylovulum* in winter (Fig. 6).

Temperature response of methane oxidation

The seasonal pattern of methanotroph succession could be controlled by temperature. To test this, temperature responses of representative samples from winter (March 12-14, 2018) and summer (August 26, 2019) were compared. The winter sample showed a psychrophilic response of methane oxidation activity, with maximal oxidation rates at 15^{o}C, while the summer sample showed a mesophilic response, with peak activity at >30^{o}C (Fig. 7). Incubation of water samples under a methane-enriched headspace at ≤4^{o}C resulted primarily in the growth of *Methylobacter*, while enrichment at ≥8^{o}C resulted primarily in the growth of *Methyloparacoccus* (Fig. 7). Enrichment at intermediate temperatures of 8-10^{o}C resulted in the growth of both strains, but slightly more *Methyloparacoccus*. These growth data, although not quantitative, demonstrate that the *Methylobacter* are more psychrophilic than *Methyloparacocccus*, but that the *Methyloparacocccus* also grow at temperatures as low as 8^{o}C and may be psychrotolerant. The genus *Methylovulum* did not enrich in this experiment, although the community analyses suggested it is also psychrophilic.

These results suggest that the methanotrophic communities in BML are temperature-adapted, with psychrophilic *Methylobacter* dominating in winter/spring versus more mesophilic *Methyloparacoccus* in summer/fall. This assumption is consistent with measured water and sediment temperatures (Fig. 3C). Water temperatures in winter range from 0^{o}C at the lake surface to 4^{o}C at the sediment interface. At the peak of summer stratification these increase to roughly 20^{o}C and 15^{o}C, respectively. The FFT deposits in the sediment are a source of heat that is slowly declining over time, and are warmer than the overlying water in the winter, possibly

accounting for the consistent prevalence of more mesophilic *Methyloparacoccus* in sediment throughout the year. Temperatures immediately below (~0.25 m) the sediment-water interface ranged from 8 to 12°C in 2013-2014 and from 5 to 11°C in 2018-2019. The magnitude of seasonal variations decreases with depth and are minimal below 5.5 m, where the average temperature is ~11°C and seasonal fluctuations are < 0.5°C (15, 16).

Discussion

BML is intensively sampled via an adaptive management program intended to determine whether EPLs are a viable strategy for land reclamation in the oil sands industry. Piggybacking on this program allowed us to assemble a dataset on methanotroph dynamics in a seasonally stratified lake that, to our knowledge, is unique in the field in its sampling intensity and duration. Most previous studies on methanotrophs in lakes have sampled only once, or a few times in a single year. Here we sampled over 5 years, in all four seasons, as often as weekly, and were therefore able to document consistent annual community dynamics.

The species composition of the methanotrophic communities and their population sizes appear to be similar to other seasonally stratified temperate and boreal lakes. The predominance of *Gammaproteobacteria* over *Alphaproteobacteria* methanotrophs is a common property of temperate, boreal, alpine, and other freshwater lakes, especially when these are nutrient- and methane-rich (24-28, 55-58). *Alphaproteobacteria* methanotrophs were always minor components of BML, including in the methane-poor epilimnion where they thrive in some other lakes (59), and in the surface sediment where they are more important in some eutrophic lakes (60). It is likely that *Methylocystaceae* and *Beijerinckiaceae* methanotrophs are more affected by

400 the salts, alkaline pH and organic pollutants in BML, as they are proposed to be less tolerant of
401 these stresses than *Gammaproteobacteria* methanotrophs (51, 61). However, the high
402 methanotroph populations and the similar species composition compared to natural lakes suggest
403 that toxicity is not a major constraint on methanotrophy. The three major methanotroph genera in
404 BML (*Methyloparacoccus*, *Methylobacter*, and *Methylovulum*) have all been identified in other
405 freshwater lakes, with either *Methyloparacoccus* or *Methylobacter* often the most prevalent
406 genus (27, 35, 56, 58, 60, 62). *Methylovulum* and *Methylobacter* species include psychrophilic
407 isolates (63, 64), and are frequently detected in low-temperature habitats (28, 36, 56, 61, 62).
408
409 Methanotrophs were frequently a predominant part of the bacterial community in the BML water
410 column, comprising from 0 up to 58% (median 2.8%) of reads in 16S rRNA gene amplicon
411 analysis of different samples. The dominance of methanotrophs within the overall microbial
412 community is similar to other seasonally stratified lakes, where methanotroph relative abundance
413 has been reported to peak as high as 11-57% (28, 35, 55, 56). Up to 5.4×10^4 (median 1.0×10^3)
414 *pmoA* gene copies mL^{-1} were detected based on qPCR. Counts of *pmoA* genes likely
415 overestimate cell counts, as most methanotrophs have 2-3 *pmoA* copies (50, 53). Therefore, we
416 estimate maximum water populations as 2.7×10^4 cells mL^{-1} (median 0.5×10^3). The maximum
417 *pmoA* gene counts in the BML water column are slightly lower than detected in several other
418 natural lake waters (peaking at 6×10^5 to 7×10^6 copies mL^{-1}) (27), and slightly lower than
419 maximum populations of methanotrophs estimated in seasonally stratified Lake Rotsee using
420 FISH (4×10^5 cells mL^{-1}) (35, 57). However, the population ranges in different samples of BML
421 and these other lakes overlap, indicating a general similarity in methanotrophic abundance.
422 Methanotrophs were much more abundant in the BML sediment than in the water column,

reaching up to 9×10^7 *pmoA* copies g^{-1} (w.w.). This quantity closely resembles that detected in natural lake sediments (58, 60, 62, 66). For example, in stratified perialpine Lake Bourget, sediment *pmoA* counts averaged about 2.5×10^7 copies g^{-1} (w.w.) (58). Greater abundances in surface sediment compared to water are typical of lakes without an anoxic water zone, such as Lake Bourget and Lake Constance (58, 66). Surface sediment should present ideal conditions for methanotrophs, where O_2 and CH_4 diffusion gradients cross.

Methanotrophs were most abundant in the water column during fall turnover and under winter ice-cover, and least abundant during summer stratification. This trend was evident in relative abundances (16S rRNA gene amplicon sequencing), absolute abundances (qPCR of *pmoA* genes), and potential methane oxidation rates. It is likely that during summer, methane oxidation occurs predominantly at the sediment-water interface and deep in the hypolimnion. As the hypolimnion is hypoxic but not anoxic (7), the methanotrophic layer should occur as close to the sediment methane source as possible. ASVs of three main genera (*Methylobacter*, *Methylovulum*, *Methyloparacoccus*) segregated seasonally and spatially. In the water column, abundances of *Methylobacter* and *Methylovulum* strains peaked in winter/spring, when the methane oxidation activity was psychrophilic, while abundances of *Methyloparacoccus* peaked in summer/fall, when the methane oxidation activity was mesophilic. Vertically, *Methyloparacoccus* sp. was also predominant below the water-sediment interface, and populations of *Methylobacter* sometimes peaked just above the interface. These data are all consistent with niche differentiation of the different methanotrophs based on temperature and on concentrations of CH_4 and O_2, although O_2 and CH_4 co-vary and are difficult to untangle. Principally, the *Methylobacter* and *Methylovulum* spp. in BML appear to be psychrophilic and adapted to high O_2/low CH_4 conditions while the

446 *Methyloparacoccus* sp. is more mesophilic and adapted to high CH_4/low O_2 concentrations.
447 Methane oxidation rates in boreal lakes and sediments usually show a weak dependence on
448 temperature, with Q_{10} values of only 1.4–2.3 (67-69). Our results suggest that one reason for this
449 weak response may be the presence of multiple methanotroph populations with different
450 temperature optima.
451
452 The methanotrophic population and activity in the BML water column increased during fall
453 turnover, when methane rich hypolimnetic water mixed with O_2 rich epilimnetic water. Although
454 some of the population increase may have been due to suspension of *Methyloparacoccus* cells
455 from the sediment, the relative abundance of this genus became much higher in the water than in
456 the sediment, which would not be expected simply from suspension of sediment bacteria. Similar
457 observations of maximum methane oxidation during fall turnover have been made in other lakes
458 (21, 29, 34, 35, 70). In the seasonally-stratified temperate Lake Rotsee, methanotrophs reached a
459 maximum relative abundance of 28% during fall turnover based on 16S rRNA gene amplicon
460 analysis, a similar dominance to BML. Methane oxidation rates and *pmoA* transcripts also
461 increased in this site during turnover (35), similar to our observations in BML. Unfortunately, we
462 were unable to sample BML during the early ice-over period, but sometime between fall
463 turnover and mid-winter the predominant *Methyloparacoccus* strain was replaced by
464 *Methylobacter* and *Methylovulum* strains in the water, and the overall methanotroph populations
465 remained high. A higher abundance of methanotrophs under ice cover compared to summer was
466 also observed in multiple Swedish lakes (27). Ice cover traps methane bubbles, allowing waters
467 to become rich in dissolved methane.
468

469 Although the present dataset is more extensive than previous studies, the discussion above
470 suggests that the temporal and spatial dynamics of methanotrophic species in BML are typical of
471 seasonally stratified northern-latitude lakes. Niche differentiation of different species, distinct
472 seasonal communities, and rapid growth during fall turnover have all been noted before, albeit
473 with less resolution. Differences between summer and winter (sub-ice) communities were
474 observed in several Swedish lakes, where different *Methylobacter* strains dominated in different
475 seasons (27). In temperate Lake Rotsee, methanotroph succession was observed during the
476 transition from summer to fall, with rapid growth of several strains including a *Methylosoma* sp.
477 during fall turnover (35). Vertical partitioning of strains was also evident in two temperate
478 stratified lakes, where *Methylobacter* and *Crenothrix* preferred the low O_2/high CH_4
479 hypolimnion, while a *Methylovulum* preferred the oxycline area with higher O_2 (28).
480
481 The similarity of BML to natural lakes is perhaps surprising, as BML is physically and
482 chemically atypical in several ways. The pH falls within the typical range of boreal lakes in
483 Canada (average 7.7, [71]), but the salinity is much greater. Conductivity in BML is 2.6 mS cm^{-1},
484 or about 5% of seawater, while other boreal lakes in Canada average only 0.166 mS cm^{-1} (71).
485 Salinity is a major factor shaping methanotroph communities (72). Furthermore, methane is
486 produced in BML from sediment-entrained hydrocarbon pollutants rather than recent organic
487 matter. Despite this, methane production rates of BML are not atypical of lakes within this
488 climatic region. Annual methane emission rates in active tailings ponds range from 30-26,000 kg
489 ha^{-1} y^{-1}, and the rate from the active pond WIP, immediately before its conversion to BML, was
490 estimated as 3300 kg ha^{-1} y^{-1} (13). The average emission rate in the 6 years after conversion of
491 this pond to the end-pit lake BML decreased to 610 kg ha^{-1} y^{-1} (14). This falls well within the

range measured in natural boreal, temperate, and arctic lakes (8-3,000 kg ha^{-1} y^{-1} [19, 20]). It is similar to emission rates from eutrophic lakes (17-290 kg ha^{-1} y^{-1} [29, 70 and references cited therein]) and other constructed reservoirs (14). The methane concentrations measured in BML water (up to 150 μM in the hypolimnion (7)) are also within the range of values reported for other boreal and temperate lakes, which range from <1 μM to over 1 mM in the hypolimnion (20, 22, 34, 56, 70, 73, 74). Therefore despite the altered chemistry compared to natural lakes, indicators of the methane cycle are similar.

When lakes are eutrophic, methanotrophy has been shown to be largely responsible for O_2 demand, accounting for as much as 60% of the total BOD (29, 31, 70). We noted that potential methane oxidation rates in BML were similar to BOD rates (data not shown), suggesting that when present, methane can account for a large amount of the oxygen demand. This assessment is consistent with previous calculations of *in situ* methane oxidation rates (7). Trapping of methane-saturated water under ice in eutrophic lakes can even result in complete lake anoxia due to methane oxidation, resulting in a “winter kill” of fish and invertebrates (29, 70). However, while winter anoxia was observed just before ice-off in 2013, it has not been noted subsequently in BML (9). The dependence of methane emissions from BML to date on atmospheric pressure changes suggests that ebullition plays a major role in methane efflux (14), and bubbling is commonly observed (8). However, as methane efflux has been declining over time (14), a higher proportion of the flux is likely to become diffusive in the future, and methanotrophs may become relatively more important for limiting methane emissions.

In summary, in this study we present one of the most extensive datasets ever assembled for lake methanotroph populations, and document consistent seasonal patterns of species dominance and turnover, likely controlled by recurring niches of particular temperatures and O_2/CH_4 concentrations created by seasonal turnover cycles. Methanotroph populations were most predominant in the water column in fall and winter. Psychrophilic *Methylobacter* and *Methylovulum* dominated methanotroph communities in winter. Conversely, more mesophilic *Methyloparacoccus* dominated in the hypolimnion during summer and in the sediment year-round, and accounted for most of the rapid overall increase in the methanotroph population throughout the water column in fall. Besides the three main genera, a variety of other species also appeared in summer, when methanotroph diversity was maximal, and may take advantage of microniches created by counter-gradients of O_2 and CH_4 during stratification. Finally, there appears to have been a gradual increase in methanotroph diversity over time as this end-pit lake has aged. This trend could be related to gradual changes in lake chemistry such as declining turbidity and salinity, or to the gradual decrease in the intensity of the methane cycle as the end-pit lake has aged (14). This trend may point to a changing ecosystem able to support higher biodiversity with time. Although comparison with previous studies is somewhat speculative because few studies have sampled as intensively at this one, biotic factors such as methanotroph community composition, potential activity, population sizes, and seasonal turnover all indicate that the methane cycle of BML is similar to that of natural seasonally stratified lakes.

Acknowledgements

This work was primarily supported by a Natural Sciences and Engineering Research Council of Canada (NSERC) Collaborative Research and Development Grant (NSERC grant

CRDPJ478071-14) in collaboration with Syncrude Canada, Ltd. EA was supported by a King Abdullah Scholarship Program (KASP), Ministry of Education, Kingdom of Saudi Arabia. SBR received support from the NERC Canada Graduate Scholarship – Master's (CGS-M) program and MBJL also acknowledges support from the NSERC CRD program (CRDPJ476388–14). We would especially like to thank Carla Wytrykush and Chris Beierling at Syncrude, Inc., and Michelle Betts at Hatfield Associates for their dedicated assistance with sampling and other issues.

Competing interests.

The authors declare no conflict of interest.

References

1. Dompierre K, Lindsay M, Cruz-Hernández P, Halferdahl G. 2016. Initial geochemical characteristics of fluid fine tailings in an oil sands end pit lake. Sci Tot Environ 556:196-206.
2. Dompierre KA, Barbour SL. 2016. Thermal properties of oil sands fluid fine tailings: laboratory and *in situ* testing methods. Can Geotech J 54:428-440.
3. Foght JM, Gieg LM, Siddique T. 2017. The microbiology of oil sands tailings: past, present, future. FEMS Microbiol Ecol 93: fix034.
4. Dompierre KA, Barbour SL. 2016. Characterization of physical mass transport through oil sands fluid fine tailings in an end pit lake: a multi-tracer study. J Contam Hydrol 189:12-26.
5. Province of Alberta. 2018. Alberta Regulation 115/93: Environmental Protection and 579 Enhancement Act: Conservation and Reclamation Regulation. Alberta Queen's Printer. Edmonton, Alberta.
6. Kabwe L, Scott JD, Beier N, Wilson G, Jeeravipoolvarn S. 2018. Environmental implications of end pit lakes at oil sands mines in Alberta. Canada. Environ Geotech 6: Paper 1700110.
7. Risacher FF, Morris PK, Arriaga D, Goad C, Nelson TC, Slater GF, Warren LA. 2018. The interplay of methane and ammonia as key oxygen consuming constituents in early stage development of Base Mine Lake, the first demonstration oil sands pit lake. Appl Geochem 93:49-59.
8. Lawrence GA, Tedford EW, Pieters R. 2015. Suspended solids in an end pit lake: potential mixing mechanisms. Can J Civ Engin 43:211-217.
9. Tedford E, Halferdahl G, Pieters R, Lawrence GA. 2019. Temporal variations in turbidity in an oil sands pit lake. Environ Fluid Mech 19:457-473.
10. Siddique T, Fedorak PM, Foght JM. 2006. Biodegradation of short-chain n-alkanes in oil sands tailings under methanogenic conditions. Environ Sci Technol 40:5459-5464.
11. Siddique T, Fedorak PM, MacKinnon MD, Foght JM. 2007. Metabolism of BTEX and naphtha compounds to methane in oil sands tailings. Environ Sci Technol 41:2350-2356.
12. Siddique T, Penner T, Semple K, Foght JM. 2011. Anaerobic biodegradation of longer-chain n-alkanes coupled to methane production in oil sands tailings. Environ Sci Technol 45:5892-5899.
13. Small CC, Cho S, Hashisho Z, Ulrich AC. 2015. Emissions from oil sands tailings ponds: Review of tailings pond parameters and emission estimates. J Petrol Sci Engin 127:490-501.
14. Clark MG, Drewitt GB, Carey SK. 2021. Energy and carbon fluxes from an oil sands pit lake. Sci Total Environ 752:141966.
15. Rudderham SB. 2019. Geomicrobiology and geochemistry of fluid fine tailings in an oil sands end pit lake. M.Sc. Thesis. University of Saskatchewan, Saskatoon, Canada.
16. Francis DJ. 2020. Examining controls on chemical mass transport across the tailings-water interface of an oil sands end pit lake. M.Sc. thesis. University of Saskatchewan, Saskatoon, Canada.
17. Arriaga D, Nelson TC, Risacher FF, Morris PK, Goad C, Slater GF, Warren LA. 2019. The co-importance of physical mixing and biogeochemical consumption in controlling water cap oxygen levels in Base Mine Lake. Appl Geochem 111:104442.

18. Wik M, Varner RK, Anthony KW, MacIntyre S, Bastviken D. 2016. Climate-sensitive northern lakes and ponds are critical components of methane release. Nat Geosci 9:99-105.
19. Sepulveda-Jauregui A, Walter Anthony KM, Martinez-Cruz K, Greene S, Thalasso F. 2015. Methane and carbon dioxide emissions from 40 lakes along a north–south latitudinal transect in Alaska. Biogeosciences 12:3197-3223.
20. Denfeld BA, Baulch HM, del Giorgio PA, Hampton SE, Karlsson J. 2018. A synthesis of carbon dioxide and methane dynamics during the ice-covered period of northern lakes. Limnol Oceanogr Lett 3:117-131.
21. Kankaala P, Huotari J, Peltomaa E, Saloranta T, Ojala A. 2006. Methanotrophic activity in relation to methane efflux and total heterotrophic bacterial production in a stratified, humic, boreal lake. Limnol Oceanogr 51:1195-1204.
22. Bastviken D, Cole JJ, Pace ML, Van de Bogert MC. 2008. Fates of methane from different lake habitats: Connecting whole-lake budgets and CH_4 emissions. J Geophys Res: Biogeosciences 113:g02024.
23. Verbeke TJ, Dedysh SN, Dunfield PF. 2019. Methanotrophy in acidic soils, including northern peatlands, p 133-156. *In* McGenity TJ (ed), Microbial Communities Utilizing Hydrocarbons and Lipids: Members, Metagenomics and Ecophysiology. Springer Verlag:Berlin.
24. Crevecoeur S, Ruiz-González C, Prairie YT, Del Giorgio PA. 2019. Large scale biogeography and environmental regulation of methanotrophic bacteria across boreal inland waters. Mol Ecol 28:4181–4196.
25. Kalyuzhnaya MG, Lapidus A, Ivanova N, Copeland AC, McHardy AC, Szeto E, Salamov A, Grigoriev IV, Suciu D, Levine SR, Markowitz VM, Rigoutsos I, Tringe SG, Bruce DC, Richardson PM, Lidstrom ME, Chistoserdova L. 2008. High-resolution metagenomics targets specific functional types in complex microbial communities. Nat Biotechnol 26:1029-1034.
26. Oswald K, Graf JS, Littmann S, Tienken D, Brand A, Wehrli B, Albertsen M, Daims H, Wagner M, Kuypers MM, Schubert CJ, Milucka J. 2017. *Crenothrix* are major methane consumers in stratified lakes. ISME J 11: 2124–2140.
27. Samad MS, Bertilsson S. 2017. Seasonal variation in abundance and diversity of bacterial methanotrophs in five temperate lakes. Front Microbiol 88:00142.
28. Mayr MJ, Zimmermann M, Guggenheim C, Brand A, Bürgmann H. 2020. Niche partitioning of methane-oxidizing bacteria along the oxygen–methane counter gradient of stratified lakes. ISME J 14:274-287.
29. Rudd J, Hamilton R. 1978. Methane cycling in a eutrophic shield lake and its effects on whole lake metabolism. Limnol Oceanogr 23:337-348.
30. Harrits SM, Hanson RS. 1980. Stratification of aerobic methane-oxidizing organisms in Lake Mendota, Madison, Wisconsin. Limnol Oceanogr 25:412-421.
31. Bédard C, Knowles R. 1997. Some properties of methane oxidation in a thermally stratified lake. Can J Fish Aquat Sci 54:1639-1645.
32. Lidstrom Mary E, Somers L. 1984. Seasonal study of methane oxidation in Lake Washington. Appl Environ Microbiol 47:1255-1260.
33. Saarela T, Rissanen AJ, Ojala A, Pumpanen J, Aalto SL, Tiirola M, Vesala T, Jäntti H. 2020. CH_4 oxidation in a boreal lake during the development of hypolimnetic hypoxia. Aquat Sci 82:19.

34. Taipale S, Kankaala P, Hahn MW, Jones RI, Tiirola M. 2011. Methane-oxidizing and photoautotrophic bacteria are major producers in a humic lake with a large anoxic hypolimnion. Aquat Microb Ecol 64:81-95.
35. Mayr MJ, Zimmermann M, Dey J, Brand A, Wehrli B, Bürgmann H. 2020. Growth and rapid succession of methanotrophs effectively limit methane release during lake overturn. Commun Biol 3:108.
36. Saidi-Mehrabad A, He Z, Tamas I, Sharp CE, Brady AL, Rochman FF, Bodrossy L, Abell GC, Penner T, Dong X, Sensen CW, Dunfield PF. 2013. Methanotrophic bacteria in oilsands tailings ponds of northern Alberta. ISME J 7:908-21.
37. Syncrude Canada, Inc. 2021. 2021 Pit Lake Monitoring and Research Report (Base Mine Lake Demonstration Summary: 2012-2020. https://era.library.ualberta.ca/items/498b3fee-e605-4e0c-88bc-f999e8d20143
38. Quinlan PJ, Tam KC. 2015. Water treatment technologies for the remediation of naphthenic acids in oil sands process-affected water. Chem Engin J 279:696-714.
39 Nanba K, King GM. 2000. Response of atmospheric methane consumption by Maine forest soils to exogenous aluminum salts. Appl Environ Microbiol 66:3674-3679.
40. Tamai N, Takenaka C, Ishizuka S. 2007. Water-soluble Al inhibits methane oxidation at atmospheric concentration levels in Japanese forest soil. Soil Biol Biochem 39:1730-1736.
41. Dompierre KA, Barbour SL, North RL, Carey SK, Lindsay MBJ. 2017. Chemical mass transport between fluid fine tailings and the overlying water cover of an oil sands end pit lake. Water Resour Res 53:4725-4740.
42. Knief C, Lipski A, Dunfield PF. 2003. Diversity and activity of methanotrophic bacteria in different upland soils. Appl Environ Microbiol 69:6703-14.
43. Klindworth A, Pruesse E, Schweer T, Peplies J, Quast C, Horn M, Glöckner FO. 2013. Evaluation of general 16S ribosomal RNA gene PCR primers for classical and next-generation sequencing-based diversity studies. Nucl Acids Res 41:e1.
44. Sheremet A, Jones GM, Jarett J, Bowers RM, Bedard I, Culham C, Eloe-Fadrosh EA, Ivanova N, Malmstrom RR, Grasby SE, Woyke T, Dunfield PF. 2020. Ecological and genomic analyses of candidate phylum WPS-2 bacteria in an unvegetated soil. Environ Microbiol 22:3143-3157.
45. Caporaso JG, Kuczynski J, Stombaugh J, Bittinger K, Bushman FD, Costello EK, Fierer N, Peña AG, Goodrich JK, Gordon JI, Huttley GA, Kelley ST, Knights D, Koenig JE, Ley RE, Lozupone CA, McDonald D, Muegge BD, Pirrung M, Reeder J, Sevinsky JR, Turnbaugh PJ, Walters WA, Widmann J, Yatsunenko T, Zaneveld J, Knight R. 2010. QIIME allows analysis of high-throughput community sequencing data. Nat Meth 7:335-336.
46. Martin M. 2011. Cutadapt removes adapter sequences from high-throughput sequencing reads. EMBnetjournal 17: 10-12.
47. Callahan BJ, McMurdie PJ, Rosen MJ, Han AW, Johnson AJ, Holmes SP. 2016. DADA2: High-resolution sample inference from Illumina amplicon data. Nat Methods 13:581-583.
48. Quast C, Pruesse E, Yilmaz P, Gerken J, Schweer T, Yarza P, Peplies J, Glöckner FO. 2013. The SILVA ribosomal RNA gene database project: improved data processing and web-based tools. Nucl Acids Res 41:D590-D596.

49. Ludwig W, Strunk O, Westram R, Richter L, Meier H, Yadhukumar, Buchner A, Lai T, Steppi S, Jobb G, Förster W, Brettske I, Gerber S, Ginhart AW, Gross O, Grumann S, Hermann S, Jost R, König A, Liss T, Lüssmann R, May M, Nonhoff B, Reichel B, Strehlow R, Stamatakis A, Stuckmann N, Vilbig A, Lenke M, Ludwig T, Bode A, Schleifer KH. 2004. ARB: a software environment for sequence data. Nucl Acids Res 32.

50. Khadka R, Clothier L, Wang L, Lim CK, Klotz MG, Dunfield PF. 2018. Evolutionary history of copper membrane monooxygenases. Front Microbiol 9:2493.

51 Dedysh SN, Dunfield PF. 2016. Family *Beijerinckiaceae*. in Whitman, W.B. (ed) Bergey's Manual of Systematics of Archaea and Bacteria 3rd Edition, vol. 1, Springer-Verlag, New York, NY.

52 Knief C. 2015. Diversity and habitat preferences of cultivated and uncultivated aerobic methanotrophic bacteria evaluated based on *pmoA* as molecular marker. Front Microbiol 6:1346.

53. Kolb S, Knief C, Stubner S, Conrad R. 2003. Quantitative detection of methanotrophs in soil by novel pmoA-targeted real-time PCR assays. Appl Environ Microbiol 69. 2423–2429.

54 Mandal S, Van Treuren W, White RA, Eggesbø M, Knight R, Peddada SD. 2015. Analysis of composition of microbiomes: a novel method for studying microbial composition. Microb Ecol Health and Dis 26:27663.

55 Martin G, Rissanen AJ, Garcia SL, Mehrshad M, Buck M, Peura S. 2021. Methylumidiphilus drives peaks in methanotrophic relative abundance in stratified lakes and ponds across northern landscapes. Front Microbiol 12:669937.

56 Rissanen AJ, Saarenheimo J, Tiirola M, Peura S, Aalto SL, Karvinen A, Nykänen H. 2018. Gammaproteobacterial methanotrophs dominate methanotrophy in aerobic and anaerobic layers of boreal lake waters. Aquat Microb Ecol 81:257-276.

57. Mayr MJ, Zimmermann M, Dey J, Wehrli B, Bürgmann H. 2020. Lake mixing regime selects apparent methane oxidation kinetics of the methanotroph assemblage. Biogeosciences 17:4247-4259.

58 Lyautey E, Billard E, Tissot N, Jacquet S, Domaizon I. 2021. Seasonal dynamics of abundance, structure, and diversity of methanogens and methanotrophs in lake sediments. Microb Ecol 82:559-571.

59 Rissanen AJ, Saarela T, Jäntti H, Buck M, Peura S, Aalto SL, Ojala A, Pumpanen J, Tiirola M, Elvert M, Nykänen H. 2021. Vertical stratification patterns of methanotrophs and their genetic controllers in water columns of oxygen-stratified boreal lakes. FEMS Microbiol Ecol 97: fiaa252.

60 Yang Y, Chen J, Tong T, Li B, He T, Liu Y, Xie S. 2019. Eutrophication influences methanotrophic activity, abundance and community structure in freshwater lakes. Sci Total Environ 662:863-872.

61 Dunfield PF. 2009 Methanotrophy in extreme environments. in J. Battista et al (eds) Encyclopedia of Life Sciences. John Wiley and Sons, Chichester. www.els.net.

62 Tsutsumi M, Kojima H, Fukui M. 2012. Vertical profiles of abundance and potential activity of methane-oxidizing bacteria in sediment of Lake Biwa, Japan. Microb Environ 27:67-71.

63 Oshkin IY, Belova SE, Danilova OV, Miroshnikov KK, Rijpstra WIC, Sinninghe Damsté JS, Liesack W, Dedysh SN. 2016. *Methylovulum psychrotolerans* sp. nov., a cold-adapted

methanotroph from low-temperature terrestrial environments, and emended description of the genus *Methylovulum*. Int J Syst Evol Microbiol 66:2417-2423.

64 Omel'chenko MV, Vasil'eva LV, Zavarzin GA, Savel'eva ND, Lysenko AM, Mityushina LL, Khmelenina VN, Trotsenko YA. 1996. A novel psychrophilic methanotroph of the genus *Methylobacter*. Microbiology 65:339-343.

65 Trotsenko YA, Khmelenina VN. 2005. Aerobic methanotrophic bacteria of cold ecosystems. FEMS Microbiol Ecol 53:15-26.

66 Rahalkar M, Deutzmann J, Schink B, Bussmann I. 2009. Abundance and activity of methanotrophic bacteria in littoral and profundal sediments of Lake Constance (Germany). Appl Environ Microbiol 75:119-126.

67 Dunfield P, knowles R, Dumont R, Moore TR. 1993. Methane production and consumption in temperate and subarctic peat soils: Response to temperature and pH. Soil Biol Biochem 25:321-326.

68 Segers R. 1998. Methane production and methane consumption: a review of processes underlying wetland methane fluxes. Biogeochemistry 41:23-51.

69 Duc NT, Crill P, Bastviken D. 2010. Implications of temperature and sediment characteristics on methane formation and oxidation in lake sediments. Biogeochemistry 100:185-196.

70 Addess JM, Effler SW. 1996. Summer methane fluxes and fall oxygen resources of onondaga lake. Lake Reservoir Manage 12:91-101.

71 Dranga SA, Hayles S, Gajewski K. 2017. Synthesis of limnological data from lakes and ponds across Arctic and Boreal Canada. Arct Sci 4:167-185.

72 Deng Y, Liu Y, Dumont M, Conrad R. 2017. Salinity affects the composition of the aerobic methanotroph community in alkaline lake sediments from the Tibetan Plateau. Microb Ecol 73:101-110.

73 Juutinen S, Rantakari M, Kortelainen P, Huttunen JT, Larmola T, Alm J, Silvola J, Martikainen PJ. 2009. Methane dynamics in different boreal lake types. Biogeosciences 6:209-223.

74 Denfeld BA, Ricão Canelhas M, Weyhenmeyer GA, Bertilsson S, Eiler A, Bastviken D. 2016. Constraints on methane oxidation in ice-covered boreal lakes. J Geophys Res: Biogeosciences 121:1924-1933.

762 **Table 1:** Potential methane oxidation rates in BML surface water (0.5 m from surface), bottom
763 water (8-11 m) and average throughout the water column on various sampling dates from
764 2015-2017. Raw data are means of measurements at three platforms (Surface and Bottom) or
765 at 3 platforms x 2-9 depths (Average Water Column). These were then averaged over multiple
766 sampling dates to give date-averaged means ± 1 SEM for each season. A significant
767 difference between the surface and bottom in summer based on an ANOVA is indicated with
768 an asterisk.
769

Season	Sample dates (n)	Methane oxidation rate, mean ± 1SEM (nmol ml^{-1} d^{-1})		
		Surface	Bottom	Average Water Column
Winter (sub-ice)	3	3.09 ± 1.90	3.88 ± 2.75	3.25 ± 2.32
Spring turnover	6	5.01 ± 0.88	4.61 ± 1.11	4.94 ± 0.70
Summer stratification	6	0.23 ± 0.49*	5.44 ± 0.92*	2.19 ± 0.34
Fall turnover	4	3.43 ± 1.07	2.81 ± 1.07	3.65 ± 1.01

770
771

772 **Figure Legends**

773

774 **Fig. 1:** Potential methane oxidation rates in BML water samples with time of year,
775 demonstrating the lower epilimnetic rates during summer stratification. All samples were
776 incubated at 20°C except winter samples, which were incubated at 5°C. Average dates of
777 spring and fall turnover are indicated. Top Panel: Samples at 0.5 m (epilimnion) and 8 m
778 (hypolimnion). Values are averages of samples from the three sampling platforms. Bottom
779 Panel: Depth-averaged rates for each of three sampling years, based on averages of × 5 depths
780 for 2015-2016 (0.5, 2, 4, 6, and 8 m) or 3 platforms × 2 depths for 2017 (0.5 and 8 m), ± 1
781 SEM. There is a significant difference between the surface and bottom in summer only, based
782 on the ANOVA shown in Table 1.

783

784 **Fig. 2:** Phylogenetic tree based on partial 16S rRNA gene sequences, showing the major
785 methanotroph ASVs detected in BML (in bold, from Supplementary Table 2), in relationship
786 to other methanotophic bacteria of the class *Gammaproteobacteria*. The tree was constructed
787 using a Neighbor-Joining algorithm with a Jukes-Cantor correction. Bootstrap values >50%
788 based on 1000 constructions are shown at the nodes. The scale bar represents 0.1 change per
789 nucleotide position.

790

791 **Fig. 3:** Relative abundances of methanotrophs in BML water as a percent of all bacteria, based
792 on 16S rRNA gene amplicon sequencing. Data are depth-averaged values throughout the
793 water column (0-12 m) for each platform, given as the mean ± 1 SEM of 3 platforms.
794 Separated epilimnetic and hypolimnetic data are presented in Supplementary Fig. 4. Panel A:

795 Relative abundance of all methanotrophs. The dashed line indicates a running average of 3
796 successive sampling dates. Panel B: Relative abundances of the three main methanotroph
797 genera. Each genus is the sum of several pooled ASVs. Panel C: Temperatures measured at 0-
798 2 m (surface) and 8-12 m (bottom), showing the timing of thermal stratification and turnover
799 events. The blue strip represents the addition of alum to the lake in 2016.
800
801 **Fig. 4**: Analysis of composition of microbiomes (ANCOM) (54) of methanotroph ASVs in
802 BML, showing the predominance of *Methyloparacoccus* and *Methylococcus* in summer and
803 autumn, versus *Methylobacter* and *Methylovulum* in winter in spring. The ASV numbers
804 correspond to Supplementary Table 2. The four seasons were delineated based on turnover
805 events (see Fig. 3C). Normalized values are results of two-step transformations: first,
806 Aitchison log-ratio of abundance of each taxon relative to the abundance of all remaining taxa
807 one at the time, then, the Mann-Whitney U is calculated on each log ratio to compare groups.
808
809 **Fig. 5:** qPCR quantification of *pmoA* genes over time as a proxy for methanotrophic bacterial
810 populations in surface (0.5 m) and bottom (0-1 m above the sediment) waters of BML from
811 2015-2019. Panel A: Universal *pmoA* assay for total methanotrophs. Panel B: Assay for
812 *Methyloparacoccus* and closely related genera. Panel C: Assay specific for *Methylobacter*,
813 *Methylovulum* and closely related genera. Data are means of three platforms ± 1 SEM. The
814 vertical strip in 2016 represents the addition of alum to the lake.
815
816 **Fig. 6:** Relative abundances of different methanotroph genera with depth in the water column
817 and across the water-sediment interface on 3 sampling dates (in March under ice cover, in

August during summer stratification, and in October during fall turnover), based on 16S rRNA gene amplicon sequencing. Depths are relative to the sediment interface. The depth of the water column at the three sample platforms varies from 9-12 m. Points represent individual samples.

Fig. 7: Temperature response of methanotrophy. Left Panel: Temperature response of methane oxidation rates in samples taken in winter or summer. Data are means of three replicates ± 1 SEM. Right Panel: Methanotrophs as a percent of the total bacterial communities based on 16S rRNA gene sequencing, after 30 d of incubation of a water sample taken on August 26, 2019 under 10% v/v methane in air at different temperatures, showing preferential enrichment of *Methylobacter* at low T (≤4^{o}C) and *Methyloparacoccus* at higher T (≥8^{o}C). Where bars are not shown they are below 1% of the total community.

Supplementary Figures for:

Seasonal dynamics of methanotrophic bacteria in a boreal oil sands end-pit lake

Emad A. Albakistani[1*], Felix C. Nwosu[1*], Chantel Furgason[1*], Evan S. Haupt[1], Angela V. Smirnova[1], Tobin J. Verbeke[1], Eun-Suk Lee[1], Joong-Jae Kim[1], Amelia Chan[1,3], Ilona A. Ruhl[1], Andriy Sheremet[1], Sarah B. Rudderham[2], Matthew B. J. Lindsay[2], and Peter F. Dunfield[#1]

[1] Department of Biological Sciences, University of Calgary, 2500 University Dr. NW Calgary AB

[2] Department of Geological Sciences, University of Saskatchewan, 114 Science Place, Saskatoon, SK, Canada

[3] Current address: National Bioenergy Center, National Renewable Energy Laboratory, Golden, CO, USA

Supplementary Fig. 1: Aerial view of Base Mine Lake, with sampling platforms indicated.

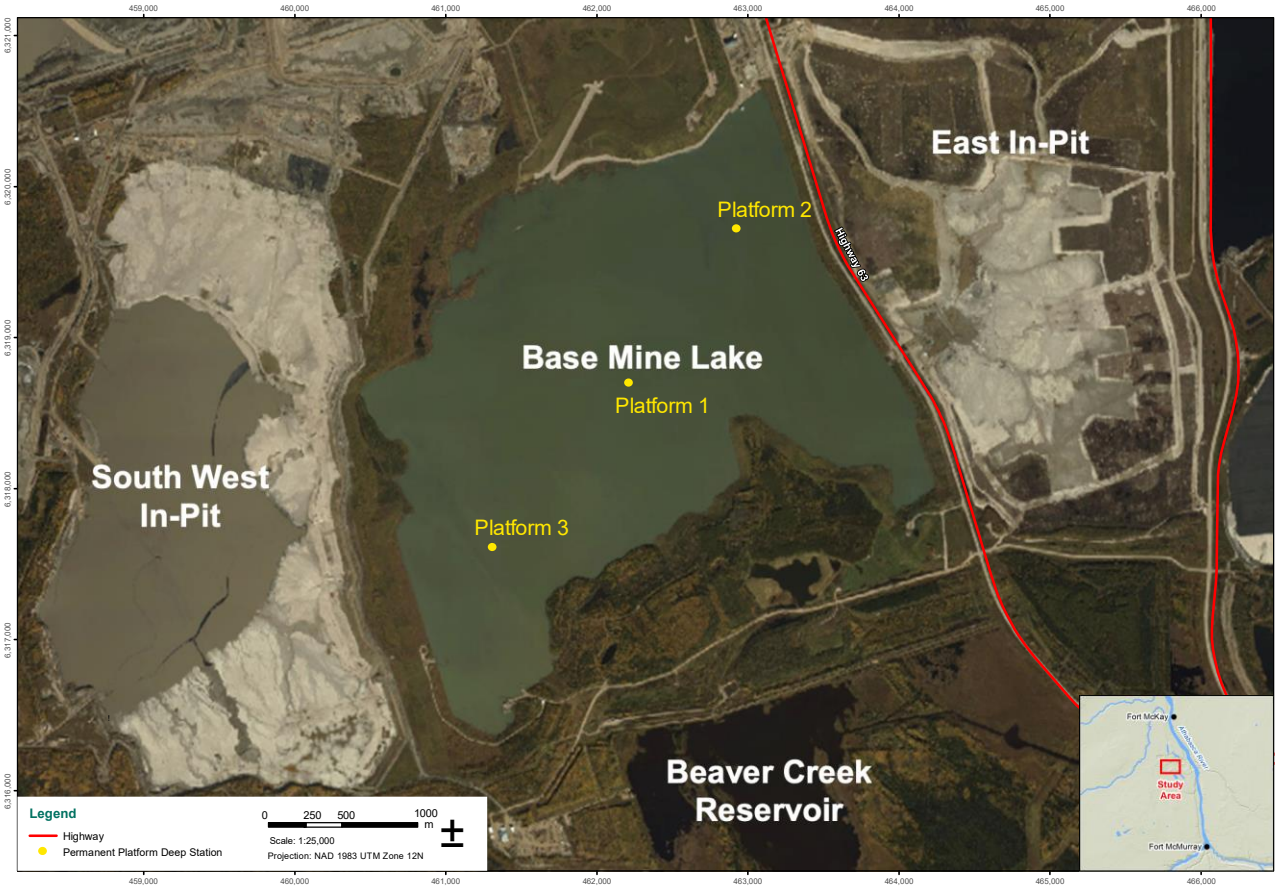

Supplementary Fig. 2: Schematic of Base Mine Lake and vertical profile (not to scale). Indicated are stratification periods in winter and summer, with the summer strata (epilimnion, metalimnion, and hypolimnion) and turnover periods in spring and autumn, indicated by arrows. The approximate depths of the water column, FFT-water interface, and the FFT layer are also indicated.

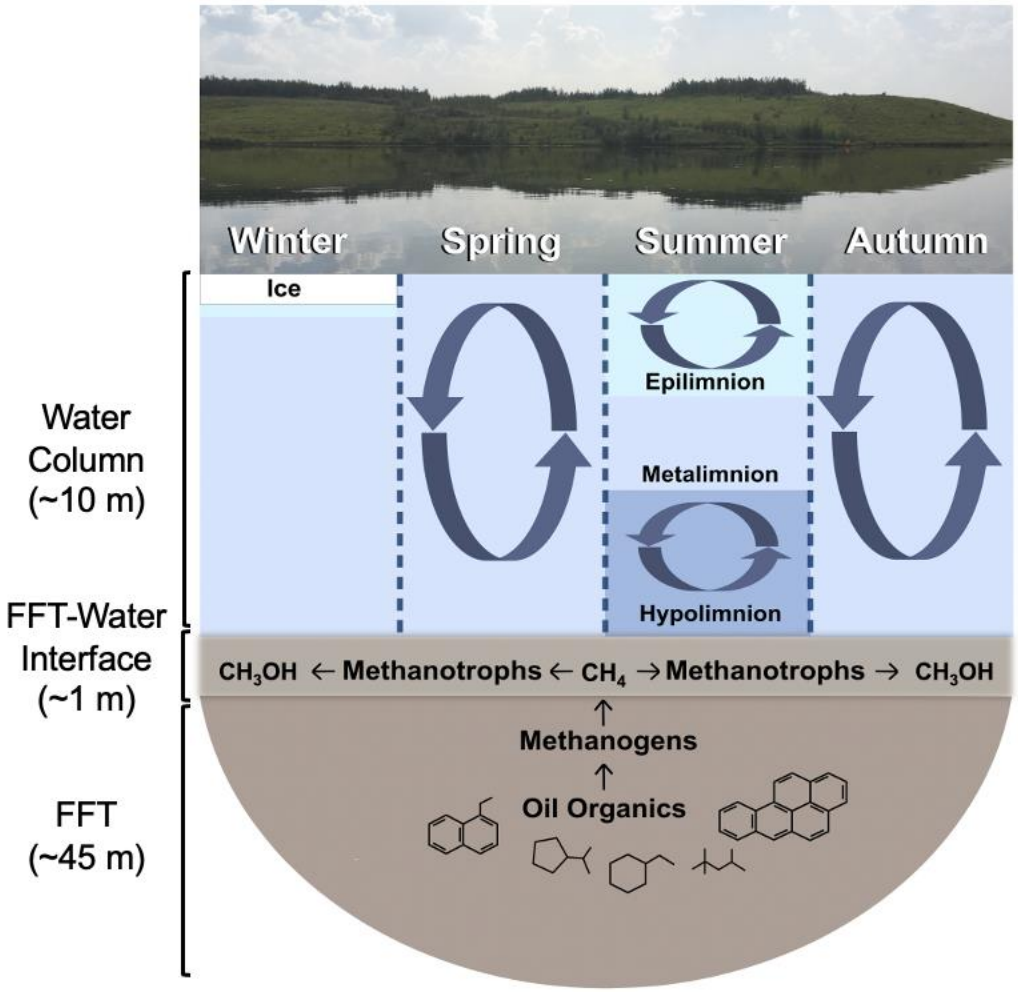

Supplementary Fig. 3: Methane oxidation rates vs depth in selected water profiles over different seasons in 2015-2017. Data are means of samples from three platforms ± 1 SEM. Measurements were made at 20ºC except for the samples received during winter (March 2015, February 2017) which were were incubated at 5°C. A strong depth effect was observed only during summer stratification. Although error bars at individual dates are large, when data from multiple dates are combined and analysed statistically, there is a significant depth effect in summer (See Table 1).

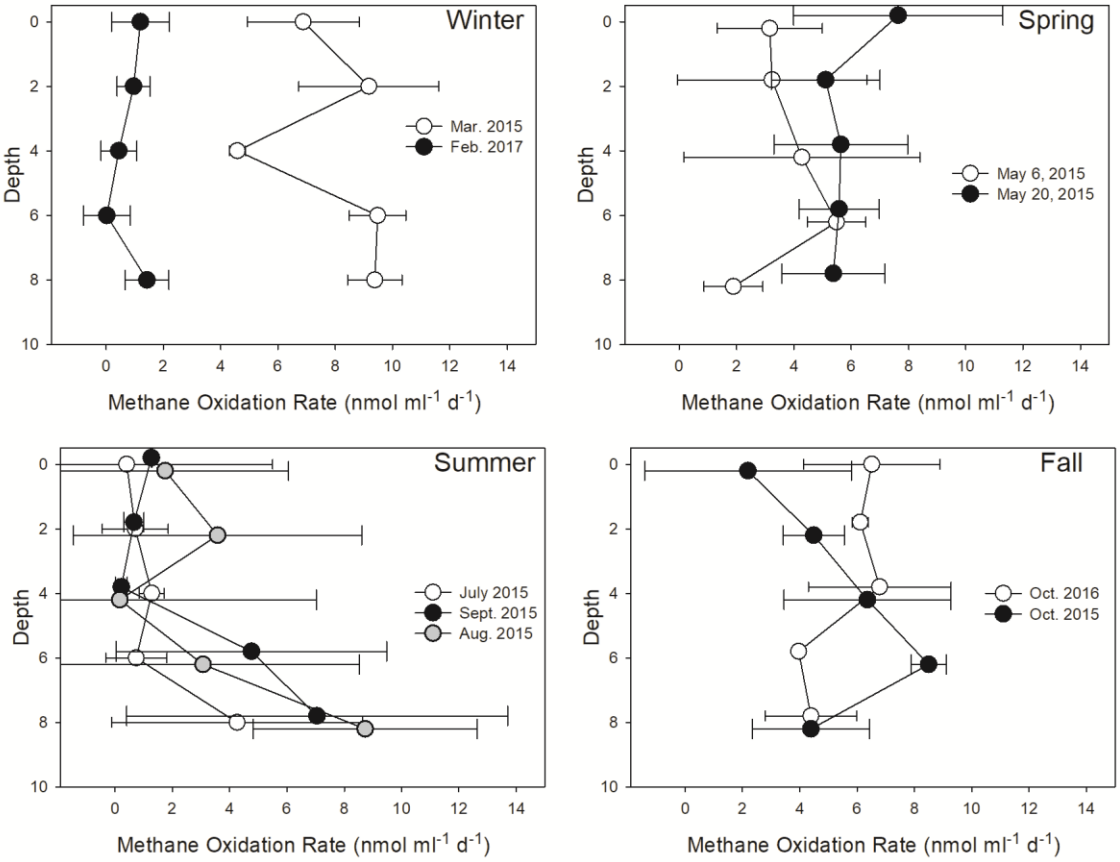

Supplementary Fig. 4: Relative abundances of methanotrophs based on 16S rRNA gene amplicon sequencing in surface (0.5 m) vs bottom (8-10 m) water samples. Points are means of samples from 3 platforms ± 1 SEM. The blue strip represents the addition of alum to the lake in 2016.

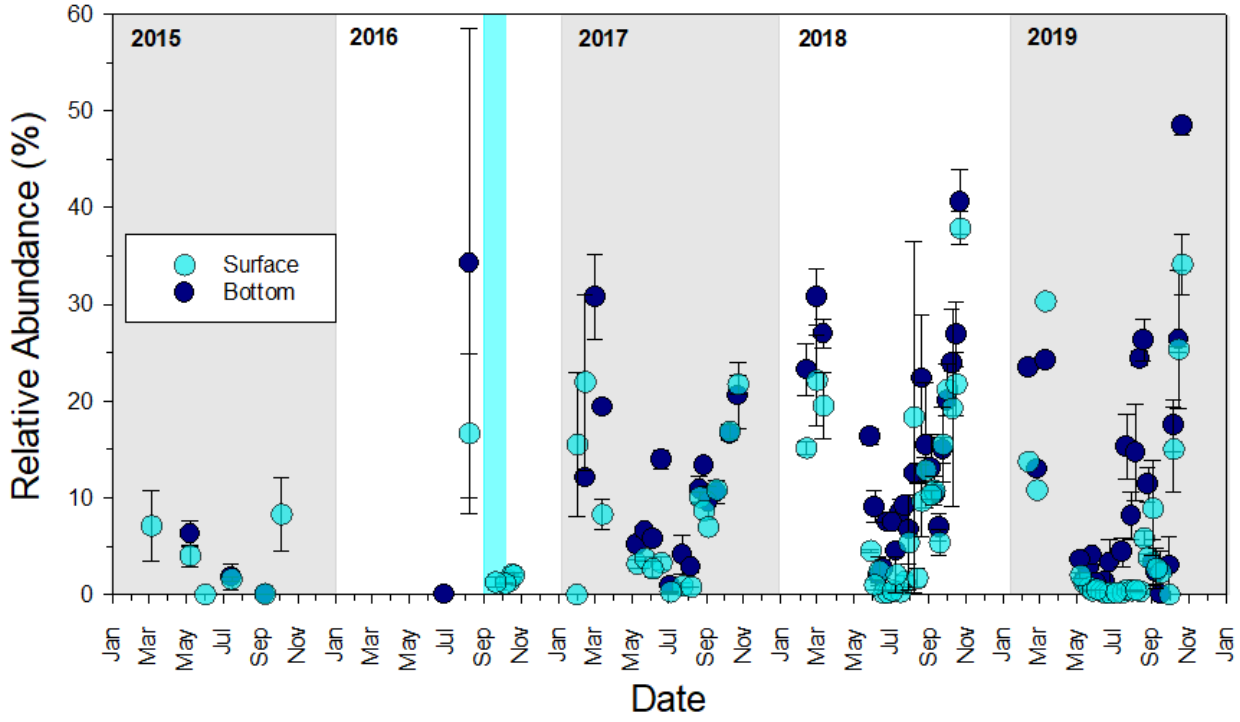

Supplementary Fig. 5: Relative abundances of the 15 main methanotroph 16S rRNA gene ASVs in BML (See Supplementary Table 4) versus time. For each platform an average of surface and bottom water samples was calculated. Data points are means of these values from 3 platforms ± 1 SEM. The blue strip represents the addition of alum to the lake in 2016.

ASV1 *Methylococcus capsulatus*

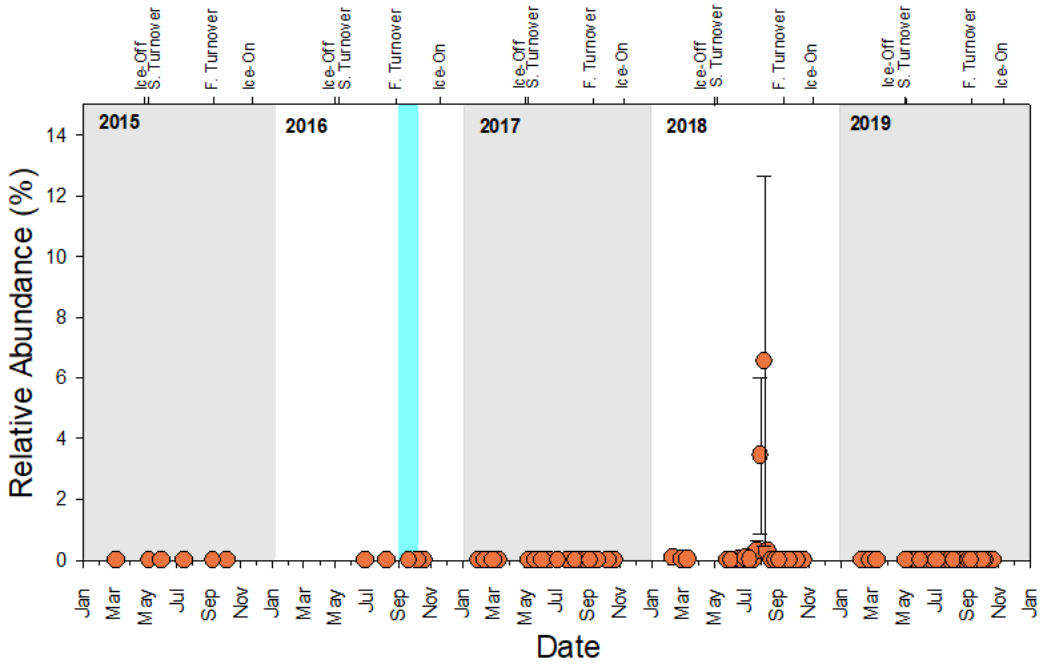

ASV2 *Methyloparacoccus* sp.

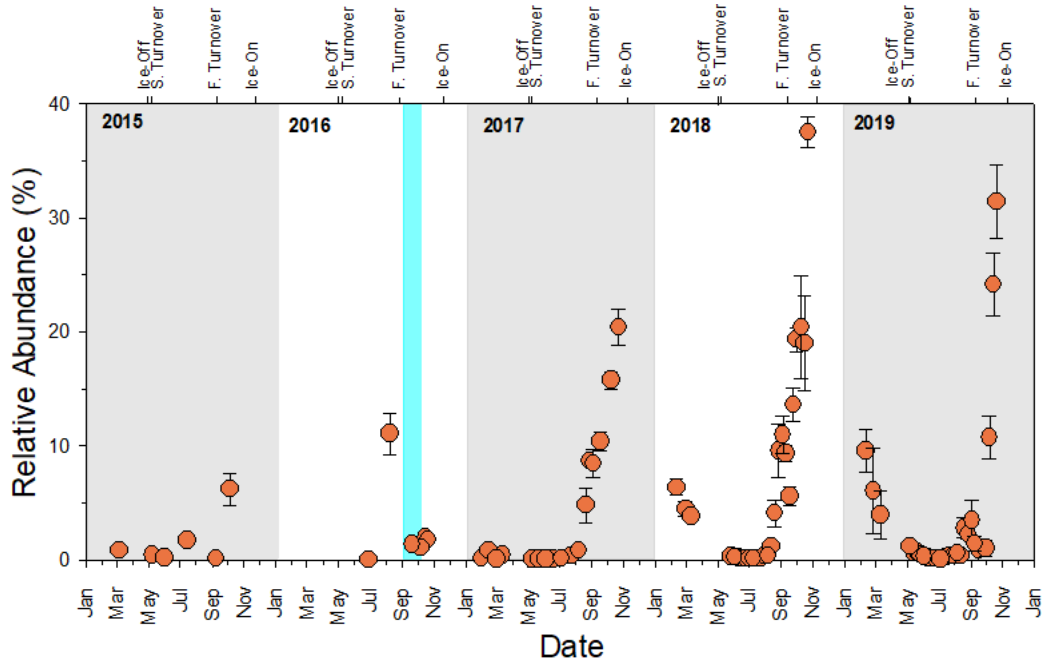

ASV3 *Methylovulum* sp.

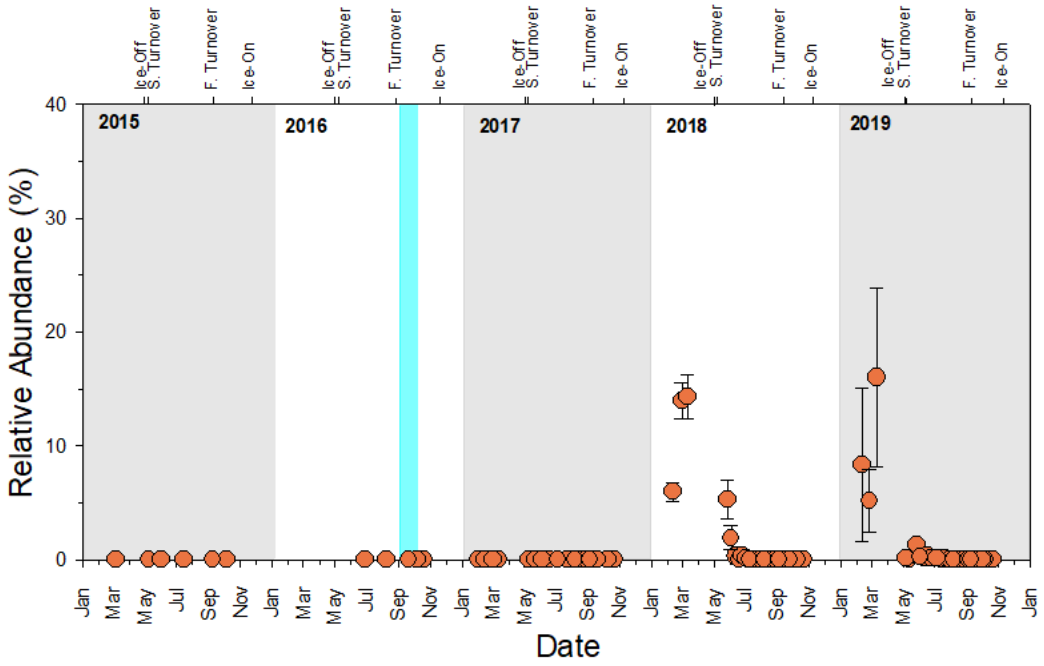

ASV4 *Methylobacter* sp.

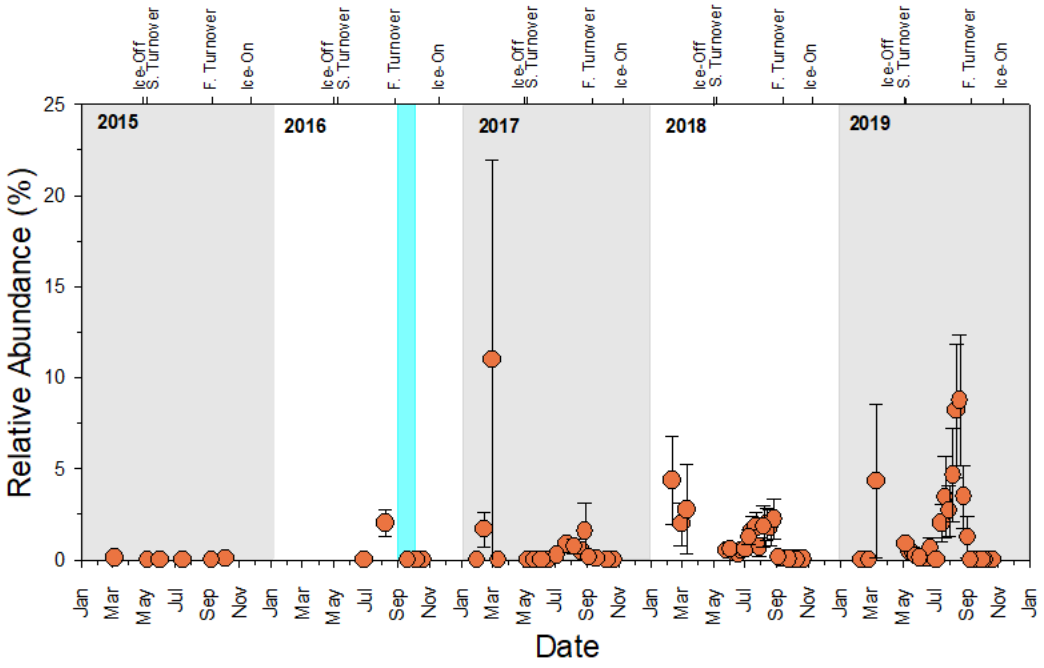

ASV5 *Methylobacter* sp.

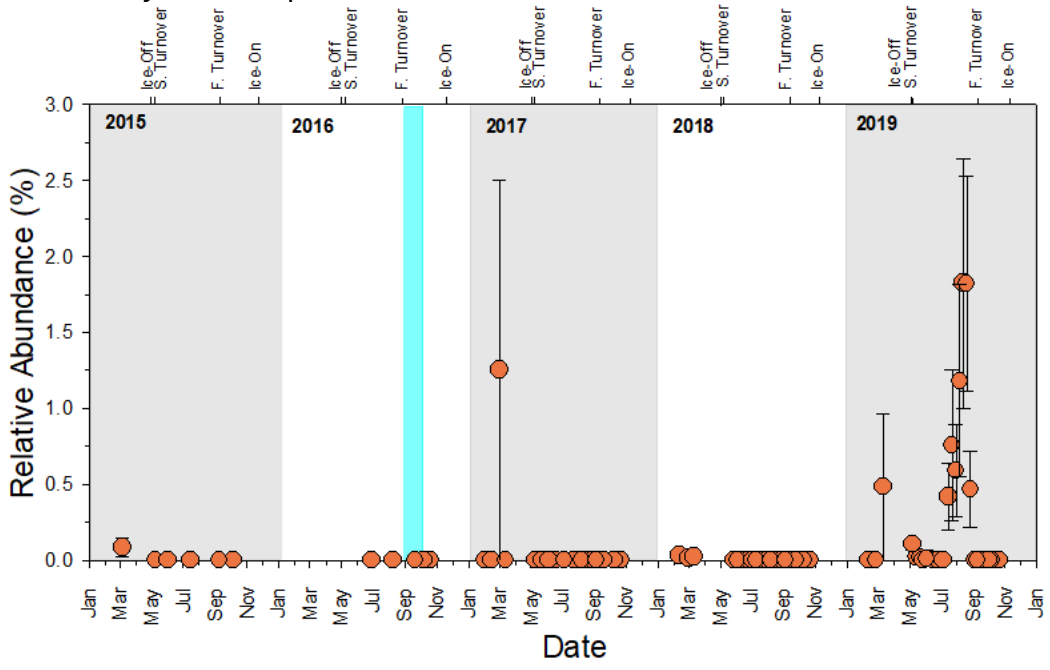

ASV6 *Methylobacter* sp.

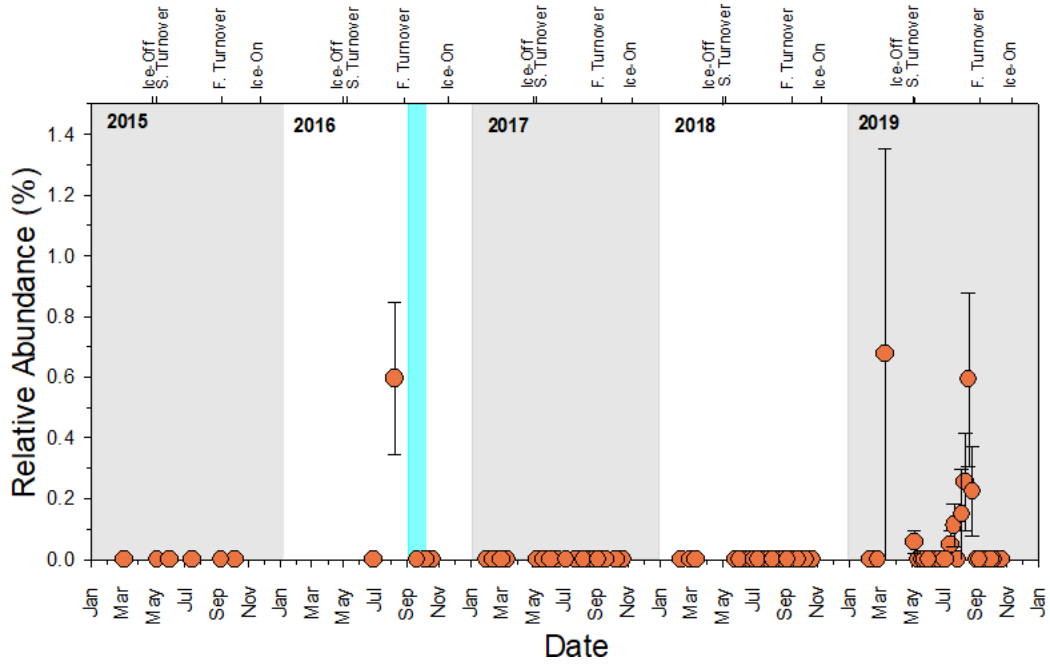

ASV7 *Methylobacter* sp.

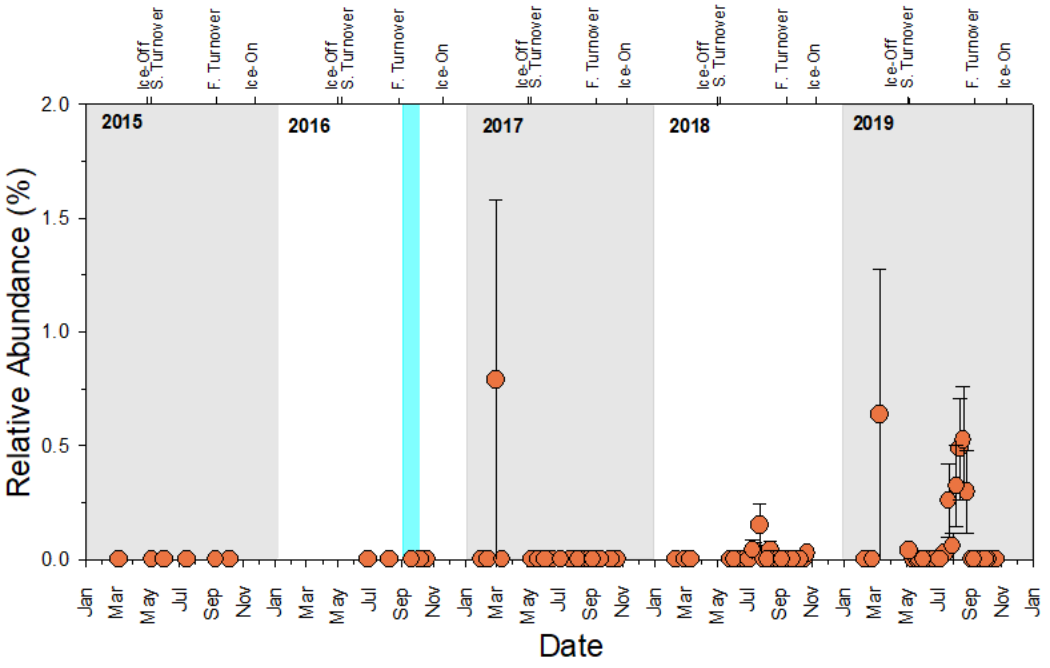

ASV8 *Methylobacter psychrophilus*

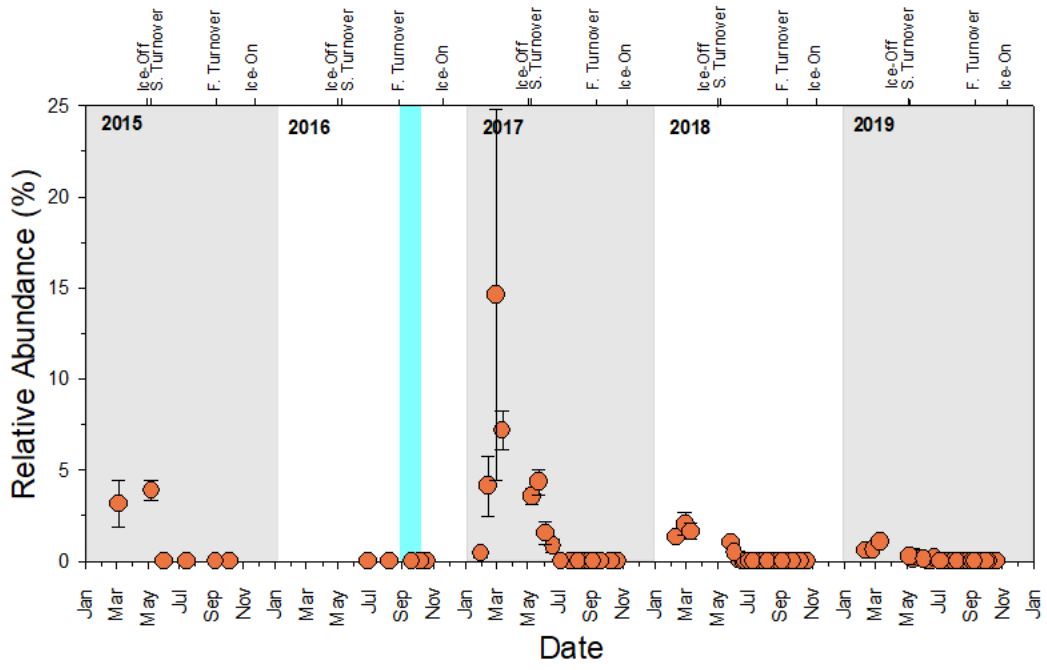

ASV9 *Methylovulum* sp.

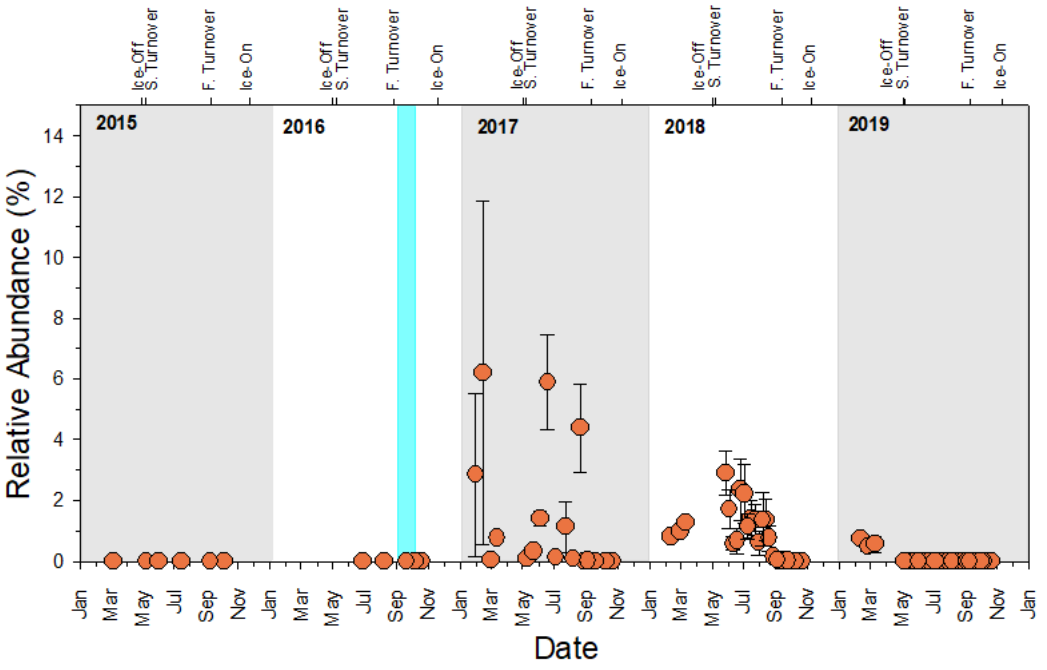

ASV10 *Methylovulum* sp.

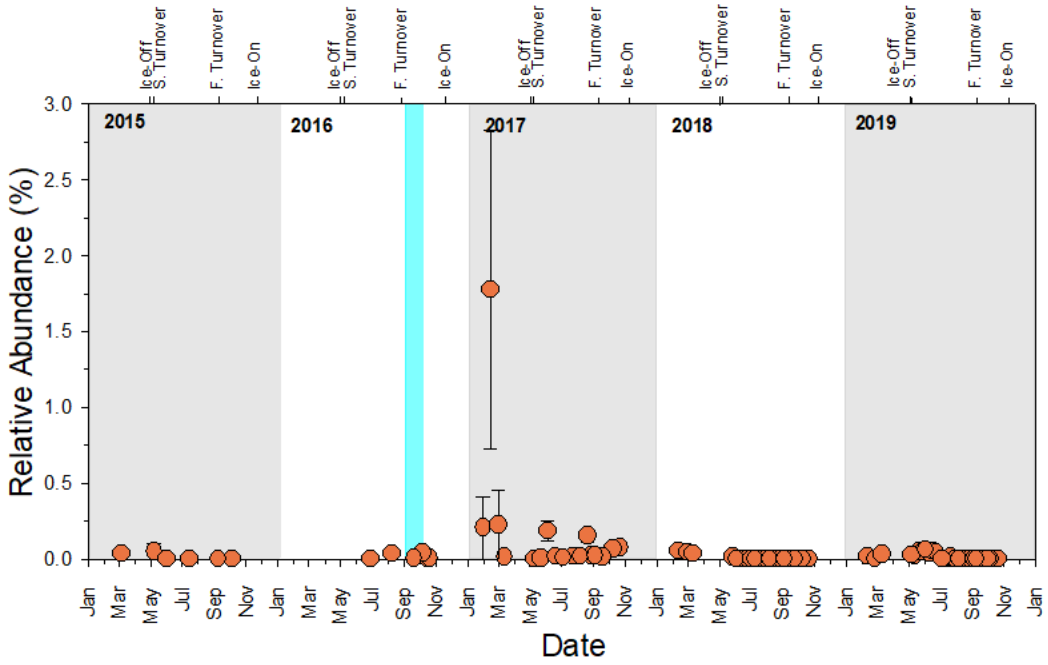

ASV11 *Methylovulum* sp.

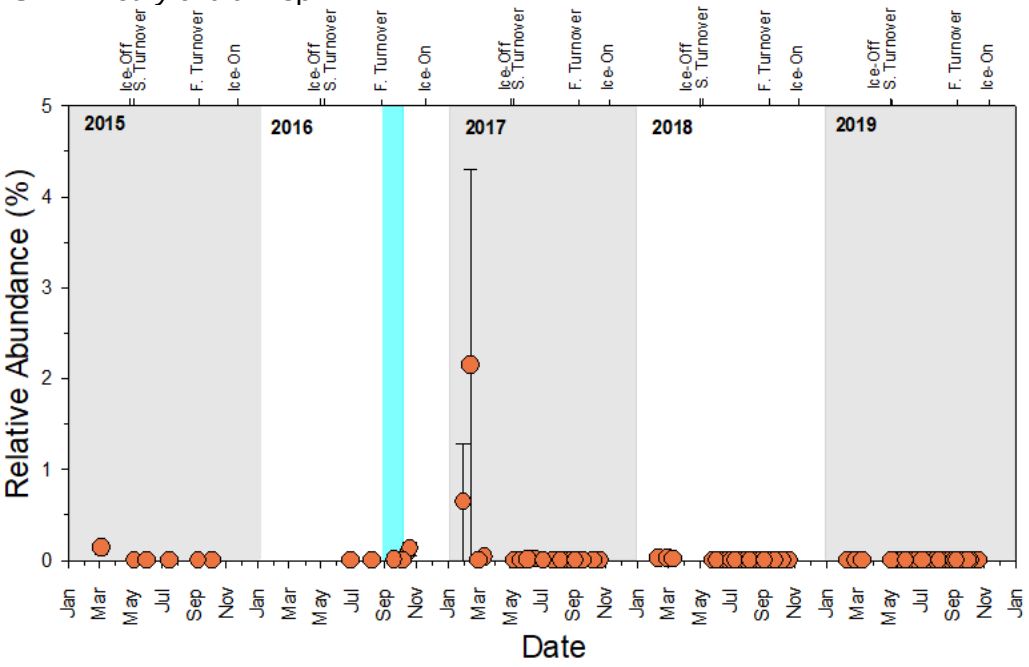

ASV12 *Methylovulum* sp.

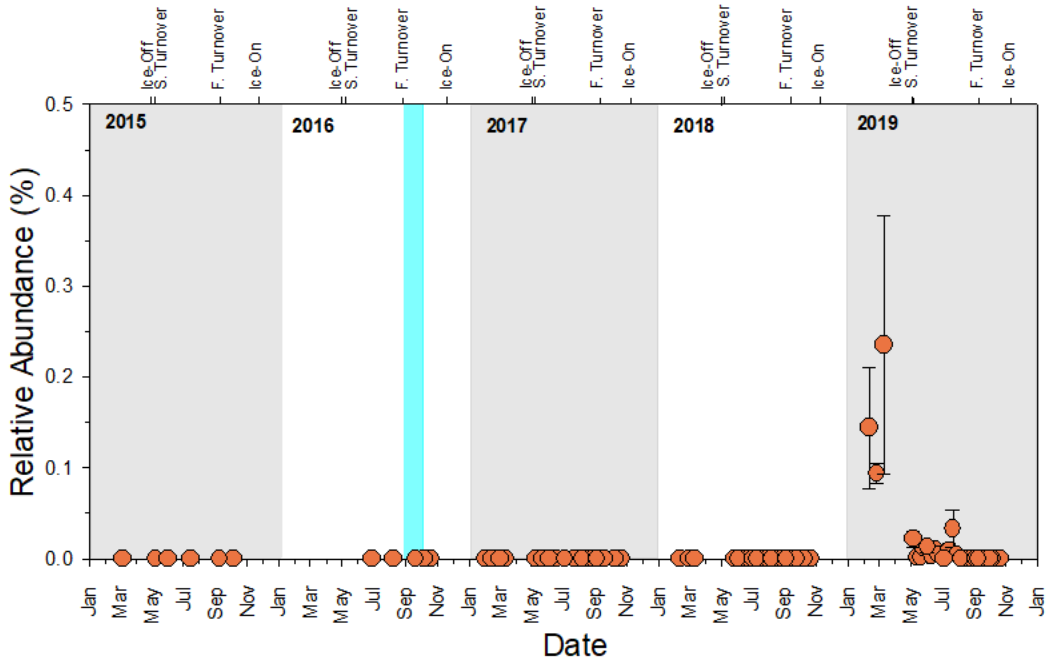

ASV13 *Methylovulum* sp.

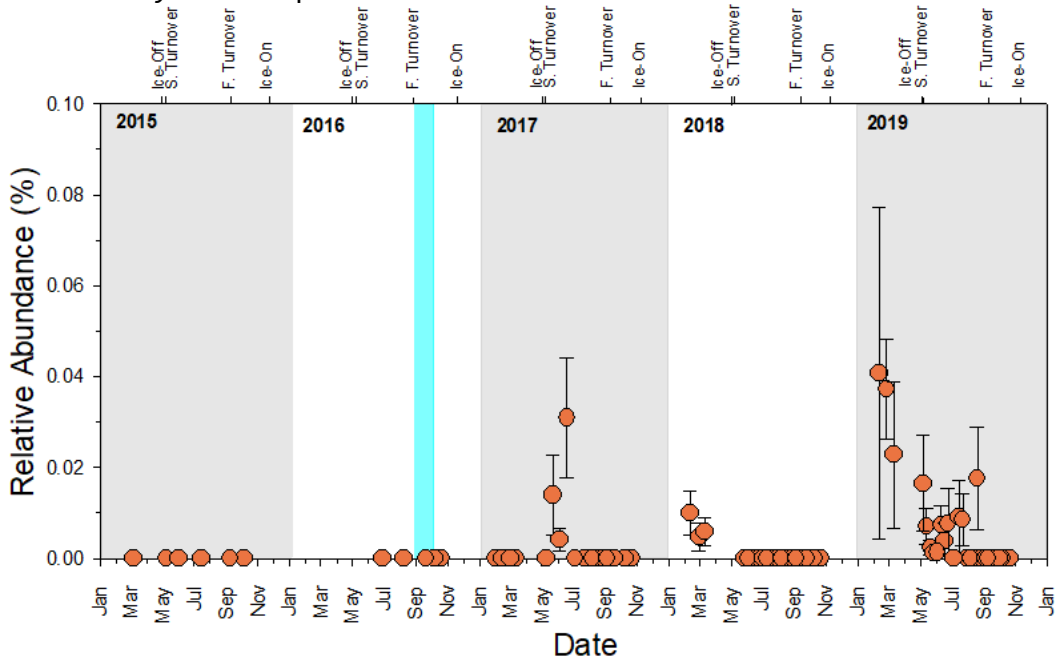

ASV14 Uncultured genus, related to *Methyloprofundus*

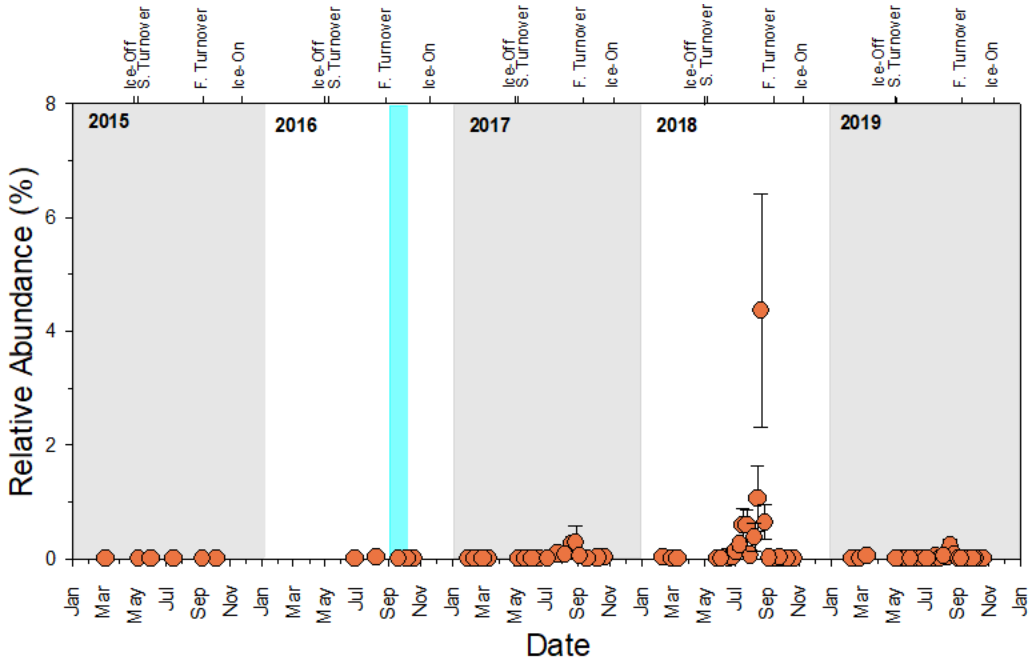

ASV15 Uncultured genus, related to *Methyloprofundus*

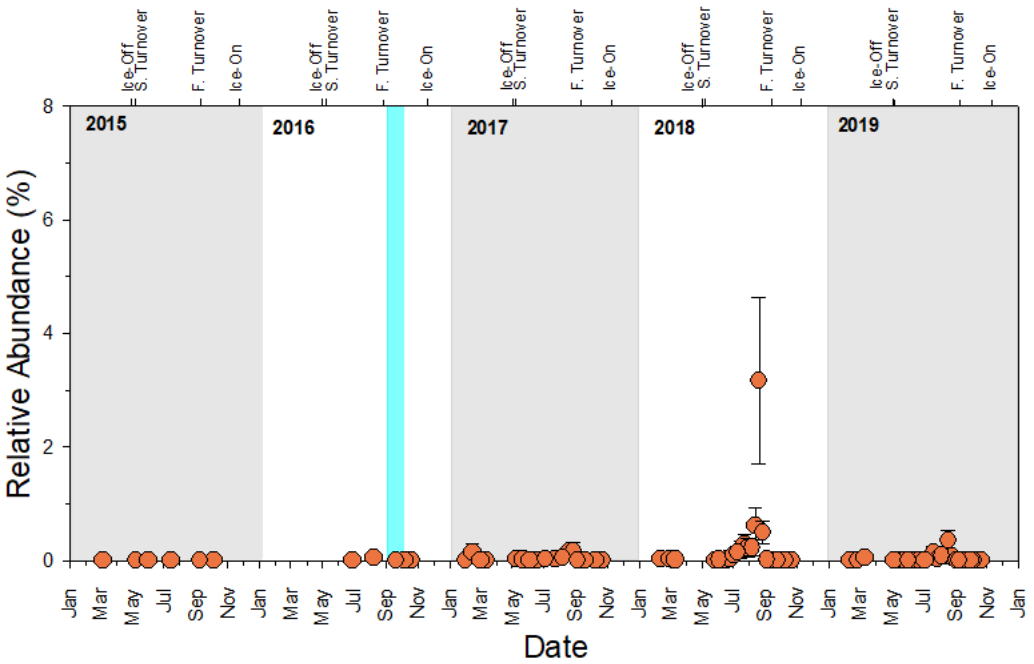

Supplementary Fig. 6: Diversity of methanotrophic bacterial communities based on Chao1 and the Shannon index. Indices were computed by selecting from the 16S rRNA gene sequencing ASV table only those ASVs identifiable as methanotrophs, and rarifying to 973 methanotrophic 16S rRNA genes reads per sample. Each point is the average of samples from 3 platforms ± 1 SEM. For each platform an average of surface and bottom water samples was calculated. The r^2 of a linear regression is shown. The blue strip represents the addition of alum to the lake in 2016.

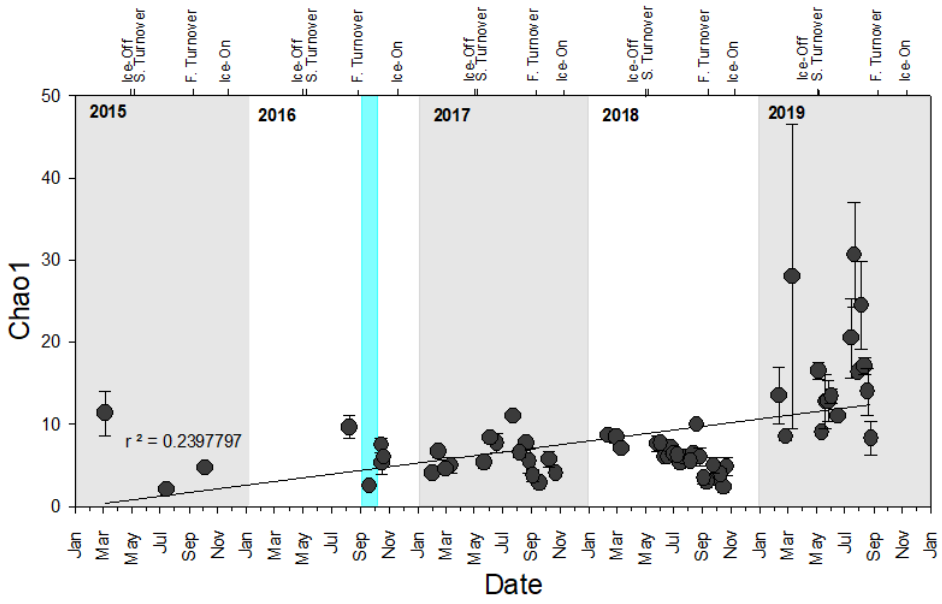

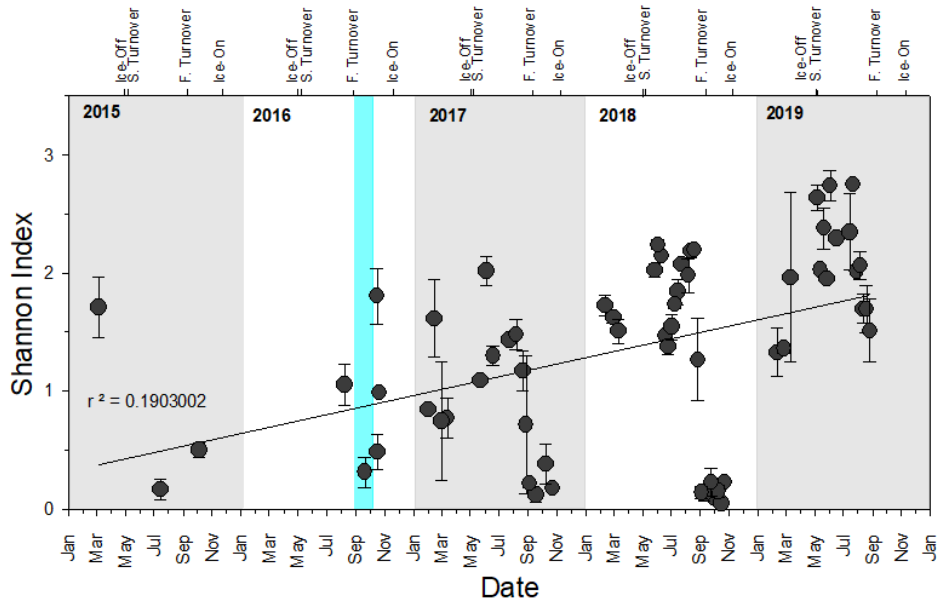

Supplementary Fig. 7: Phylogenetic tree based on partial *pmoA* gene sequences, showing *pmoA* genes detected in BML metagenomes, or from a methanotroph isolated from BML in relationship to *pmoA* gene sequences of other gammaproteobacterial methanotrophs. The tree was constructed using using a Maximum Likelihood algorithm (General Reversible Model) with 1000 bootstraps. Bootstrap values >50% are shown at the nodes. The scale bar represents 0.1 change per nucleotide position.

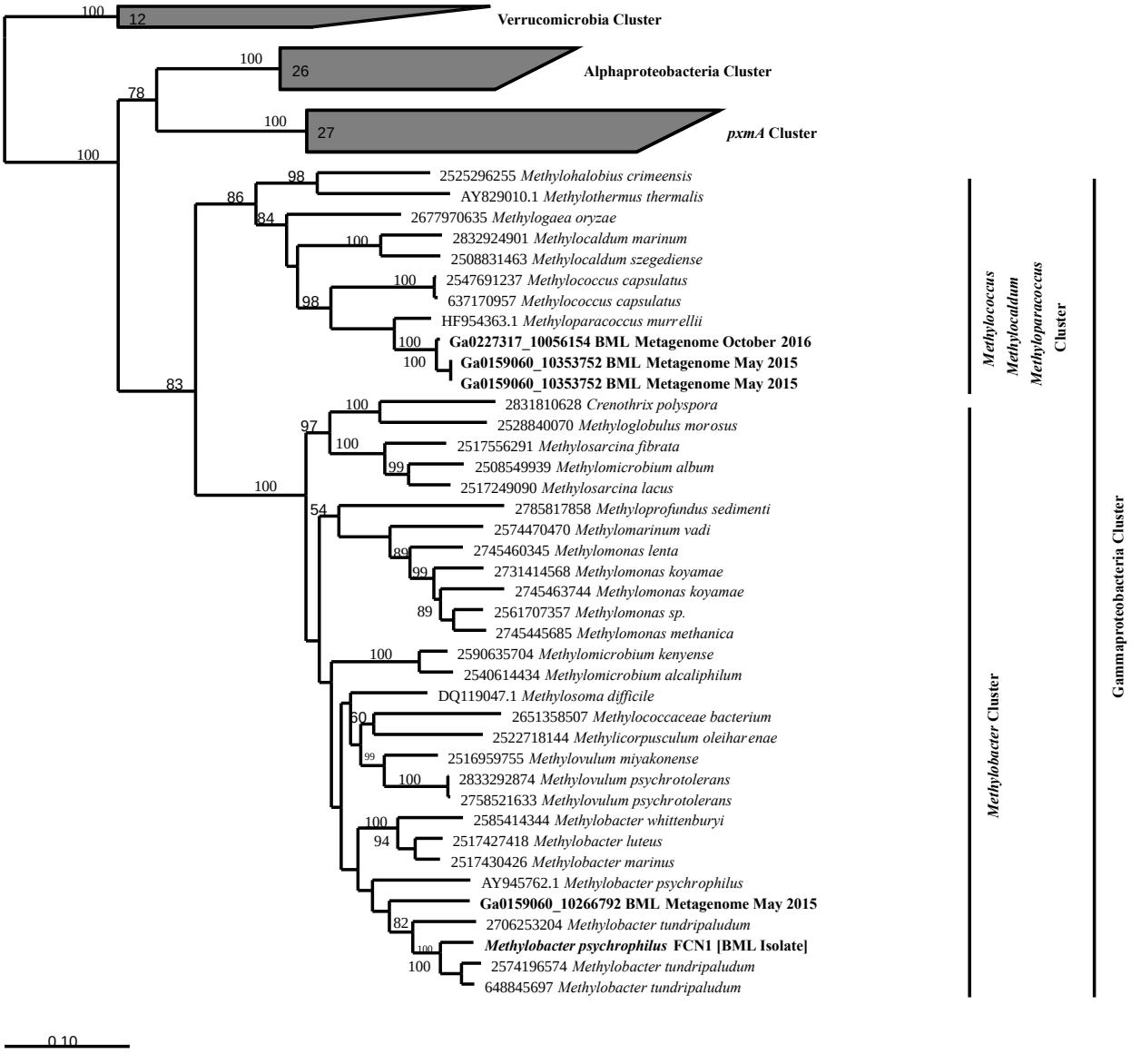

Supplementary Fig. 8: Relative abundance of some putative methylotrophs belonging to the order *Methylophilales* in BML water, as a percent of all bacteria, based on 16S rRNA gene amplicon sequencing. Top Panel: Relative abundances of three individual taxa. OM43 is a clade of the order *Methylophilales*. Bottom Panel: Combined abundance of the three taxa in the Top Panel. Most members of the *Methylophilales* are known methylotrophs (Lidstrom *et al.*, 2006; Lapidus *et al.,* 2011; Jimenez-Infante *et al*., 2016) and a previous stable isotope probing study demonstrated the assimilation of labelled $^{13}CH_4$ (probably via intermediate ^{13}C-methanol) by members of this order in water from active oilsands tailings ponds (Saidi-Mehrabad *et al.*, 2013).

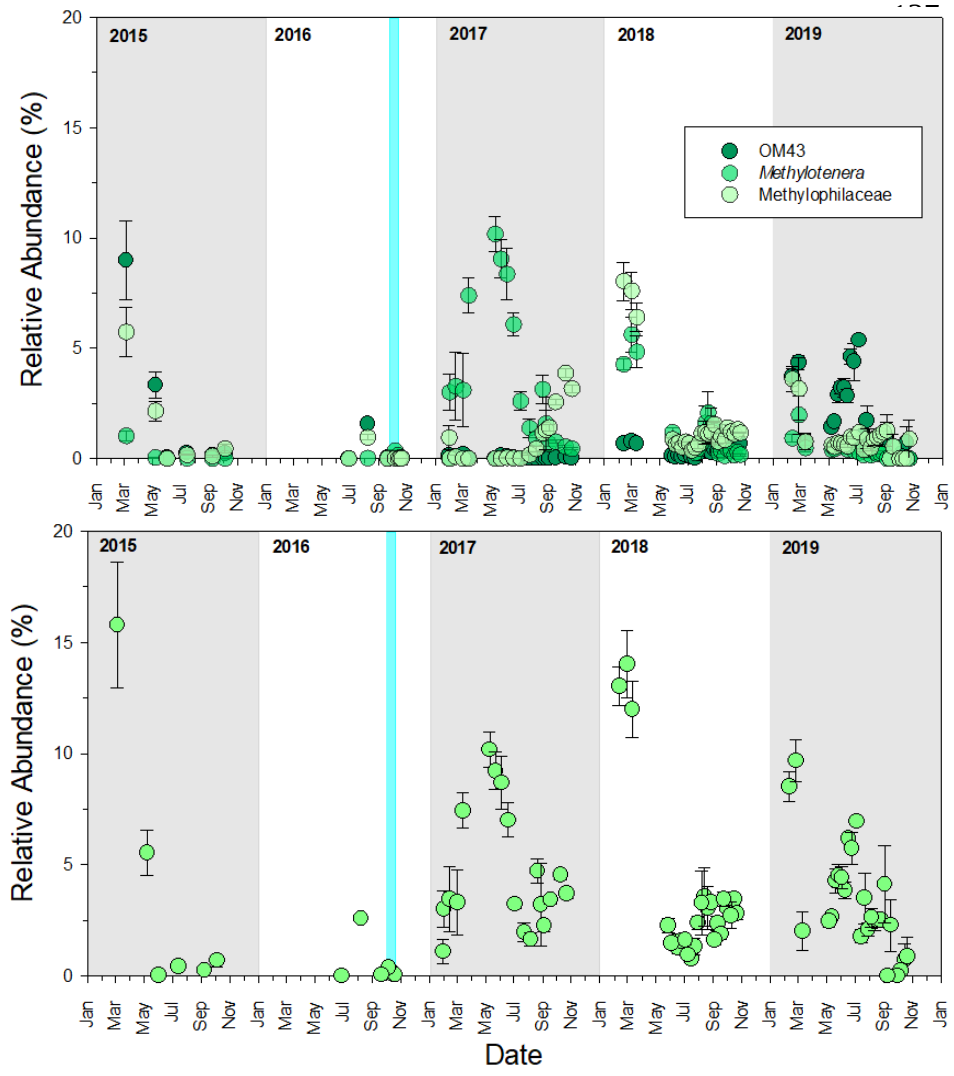

Suppplementary Fig. 9: qPCR counts of *pmoA* genes in surface tailings sediments (0-100 cm below the FFT interface) compared to water (average of all depths 0-12 m) on 4 different sampling dates. Data are in *pmoA* gene copies mL^{-1} sediment or water. Each symbol represents the average of samples from multiple depths below a single platform, and are means ± 1 SEM (n = 2 to 12 for water and n = 3 to 16 for sediment).

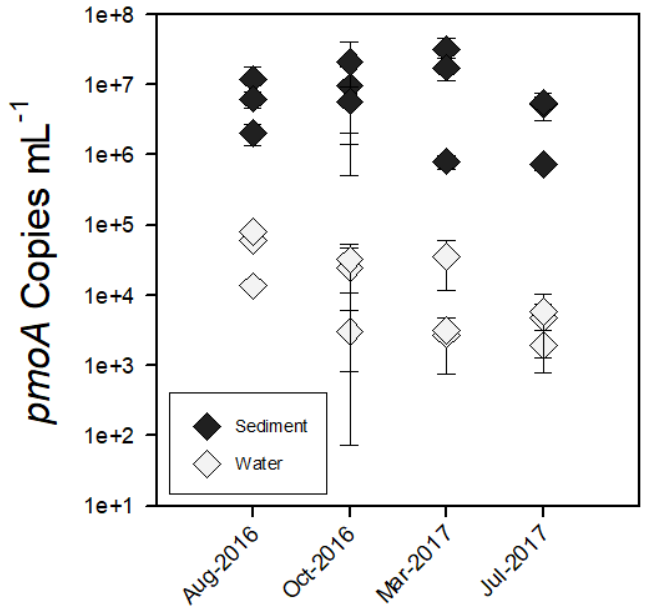

Supplementary References:

Dedysh SN, Dunfield PF. 2014. Cultivation of methanotrophs. in McGenity, T., Timmis, K., and Nogales, B. (eds) Hydrocarbon and Lipid Microbiology Protocols. Springer Protocols Handbooks. Springer-Verlag Berlin Heidelberg (www.springerprotocols.com). pp 231-247. Online resource. doi: 10.1007/8623_2014_14.

Jimenez-Infante F, Ngugi DK, Vinu M, Alam I, Kamau AA, Blom J, Bajic VB, Stingl U. 2016. Comprehensive genomic analyses of the OM43 clade, including a novel species from the Red Sea, indicate ecotype differentiation among marine methylotrophs. Appl Environ Microbiol 82:1215-1226.

Lidstrom ME.2006. Aerobic methylotrophic prokaryotes, p. 618–634. In A Balows, HG Truper, M Dworkin, W Harder, and KH Schleifer (ed.) The Prokaryotes. Springer-Verlag, New York, NY.

Lapidus A, Clum A, LaButti K, Kaluzhnaya MG, Lim S, Beck DAC, Glavina del Rio T, *et al*. 2011. Genomes of three methylotrophs from a single niche reveal the genetic and metabolic divergence of the *Methylophilaceae.* J Bacteriol 193: 3757-3764.

Supplementary Table 1: Extraction procedures for water and sediment samples

Sample	Amount processed	Centrifuge (× g)	Centrifuge time (min)	Elution Volume	Notes	Details
Water Samples 2015	160 mL	8,000	10	50 µL	40 mL run per centrifugation	Water samples were centrifuged at 8,000 × g in a Beckman Coulter Avanti® J-E centrifuge at 4°C in a JA-14 rotor (Beckman Coulter). The desired volume was reached by centrifuging 40 mL of each sample in a 50-mL Falcon tube for 10 minutes, discarding the supernatant using an automatic pipette, then adding an additional 40 mL of sample water, repeating to a total of four centrifugations per sample. After the final centrifugation, approximately 500 µL of supernatant was retained along with the pellet to resuspend the cells for transfer to 2-mL Lysing Matrix E tubes (MP BIO) for DNA extraction.
Water Samples 2016-2019	500 mL	8,000	10	25 - 80 µL	250 mL run per centrifugation	Water samples were centrifuged at 8,000 × g in a Beckman Coulter Avanti® J-E centrifuge at 4°C in a JA-14 rotor (Beckman Coulter). The desired volume was reached by centrifuging 250 mL of each sample in a 300-mL centrifuge tube for 10 minutes, discarding the supernatant, then adding an additional 250 mL of sample water and repeating. After the second centrifugation, approximately 500 µL of supernatant was retained along with the pellet to resuspend the cells for transfer to 2-mL Lysing Matrix E tubes (MP BIO) for DNA extraction.
Water-FFT Interface	20 mL	8,000	10	500 µL		For murky water at the water-FFT interface, 20-mL samples were centrifuged at 8,000 × g in a Beckman //Coulter Avanti® J-E centrifuge at 4°C in a JA-14 rotor (Beckman Coulter), in 50-mL Falcon tubes for 10 minutes. After the centrifugation, approximately 500 µL of supernatant was retained along with the pellet to resuspend the cells for transfer to 2-mL Lysing Matrix E tubes (MP BIO) for DNA extraction.
Sediment	0.5 g	3300-8000	40	25-150 µL		Sediment samples (0.5 g) were processed in two ways to ensure that inhibitory compounds did not interfere with PCR and qPCR. Similar qPCR counts were obtained for each extract. Sediments were either: A) centrifuged at 8,000 × g in a Prism R™ Refrigerated Micro Centrifuge in a 24 x 1.5 / 2.0 mL rotor, transferred into 2-mL Lysing Matrix E tubes (MP BIO), and the pellet stored at -80°C until extraction. DNA was extracted as described in the methods. or B) centrifuged at 3,300 × g for 40 minutes and the pellet stored at -20°C until extraction. DNA was extracted as described in the methods, except that cell disruption steps were repeated twice and the resulting product was pooled before adding the binding matrix solution. The ethanol wash step was repeated three times to ensure organics had been washed away. Finally, DNA was eluted twice with deoxyribonuclease-free water to obtain a final volume ranging from 100 to 150 µL.

Supplementary Table 2: The 15 major methanotroph ASVs detected in BML water samples, with number of samples (of 624 total) they were detected detected in, average abundance across all samples, maximum abundance in any single sample, and taxonomic affiliation.

MEAN	MAX	Number of Samples	ASV ID	ASV	Corrected taxonomy (genus or species)	Silva taxonomy
0.091	30.864	30	e7be86cadb06dbb89bd830c4b0d11d95	ASV 1	*Methylococcus*	D_0__Bacteria;D_1__Proteobacteria;D_2__Gammaproteobacteria;D_3__Methylococcales;D_4__Methylococcaceae;D_5__Methylococcus;D_6__Methylococcus capsulatus str. Texas = ATCC 19069
4.051	41.203	501	7a8cf7a454851bc1e87a198e98337b5f	ASV 2	*Methyloparacoccus*	D_0__Bacteria;D_1__Proteobacteria;D_2__Gammaproteobacteria;D_3__Methylococcales;D_4__Methylococcaceae;D_5__Methyloparacoccus
1.141	30.272	121	3dad610cea97b5eeb7bf78277f5295e5	ASV 3	*Methylovulum/Methylosoma*	D_0__Bacteria;D_1__Proteobacteria;D_2__Gammaproteobacteria;D_3__Methylococcales;D_4__Methylomonaceae
0.929	41.901	225	d887473e4aef78d83c4a3589b3349c95	ASV 4	*Methylobacter*	D_0__Bacteria;D_1__Proteobacteria;D_2__Gammaproteobacteria;D_3__Methylococcales;D_4__Methylomonaceae;D_5__Methylobacter
0.075	4.022	44	05aa7c6273f8ce45d225d558d5b33a4b	ASV 5	*Methylobacter*	D_0__Bacteria;D_1__Proteobacteria;D_2__Gammaproteobacteria;D_3__Methylococcales;D_4__Methylomonaceae;D_5__Methylobacter
0.039	4.800	22	fa0a74bc28c6e5baa6fba87cc0f69dbd	ASV 6	*Methylobacter*	D_0__Bacteria;D_1__Proteobacteria;D_2__Gammaproteobacteria;D_3__Methylococcales;D_4__Methylomonaceae;D_5__Methylobacter
0.026	1.579	28	9d060d311d1c69174d529d40255e4698	ASV 7	*Methylobacter*	D_0__Bacteria;D_1__Proteobacteria;D_2__Gammaproteobacteria;D_3__Methylococcales;D_4__Methylomonaceae;D_5__Methylobacter
0.743	24.821	187	acf2f44f95916d3467454eee25b06cec	ASV 8	*Methylobacter psychrophilus*	D_0__Bacteria;D_1__Proteobacteria;D_2__Gammaproteobacteria;D_3__Methylococcales;D_4__Methylomonaceae;D_5__Methylobacter;D_6__uncultured Methylococcales bacterium
0.481	23.181	198	22846b7cf88117870b0700c7f6e5b195	ASV 9	*Methylovulum/Methylosoma*	D_0__Bacteria;D_1__Proteobacteria;D_2__Gammaproteobacteria;D_3__Methylococcales;D_4__Methylomonaceae;D_5__Methylovulum;D_6__uncultured bacterium
0.032	4.102	130	82d36431a7899129ee6c31db092ec657	ASV 10	*Methylovulum/Methylosoma*	D_0__Bacteria;D_1__Proteobacteria;D_2__Gammaproteobacteria;D_3__Methylococcales;D_4__Methylomonaceae;D_5__Methylovulum;D_6__uncultured bacterium
0.028	8.596	49	4bc3779d1f12666780c4bf30cbf1ba70	ASV 11	*Methylovulum/Methylosoma*	D_0__Bacteria;D_1__Proteobacteria;D_2__Gammaproteobacteria;D_3__Methylococcales;D_4__Methylomonaceae;D_5__Methylovulum;D_6__uncultured bacterium
0.003	0.377	32	1a2ec4223878af2bb57a8f8110b9c41d	ASV 12	*Methylovulum/Methylosoma*	D_0__Bacteria;D_1__Proteobacteria;D_2__Gammaproteobacteria;D_3__Methylococcales;D_4__Methylomonaceae;D_5__Methylovulum;D_6__uncultured bacterium
0.002	0.085	55	e8abc9fe20f9c0c5c5f196e08eb7ad9a	ASV 13	*Methylovulum/Methylosoma*	D_0__Bacteria;D_1__Proteobacteria;D_2__Gammaproteobacteria;D_3__Methylococcales;D_4__Methylomonaceae;D_5__Methylovulum;D_6__uncultured bacterium
0.088	10.253	73	348f7df88c25251109fe24b5a301a5ff	ASV 14	uncultured *Methyloprofundus*-like	D_0__Bacteria;D_1__Proteobacteria;D_2__Gammaproteobacteria;D_3__Methylococcales;D_4__Methylomonaceae;D_5__uncultured;D_6__uncultured bacterium
0.066	7.132	82	aa4510180c5b33f4a8aa91e0d38f831f	ASV 15	uncultured *Methyloprofundus*-like	D_0__Bacteria;D_1__Proteobacteria;D_2__Gammaproteobacteria;D_3__Methylococcales;D_4__Methylomonaceae;D_5__uncultured;D_6__uncultured bacterium

Supplementary Table 3: Details of the metagenomes from BML water that were generated in order to obtain full-length *pmoA* gene sequences.

Sample	Library prep	sequencing	assembly	Mb	N50	JGI Analysis project ID	JGI Sequencing Project ID
BML May 2015	NexteraXT DNA Library Prep Kit	Illumina MiSeq	4.SPAdes-3.8.0-Linux	195.1	1249	Ga0159060	Gp0053501
BML October 2016	NexteraXT DNA Library Prep Kit	Illumina MiSeq	4.SPAdes-3.8.0-Linux	106.5	1740	Ga0227317	Gp0266534
BML March 2017	NexteraXT DNA Library Prep Kit	Illumina MiSeq	4.SPAdes-3.8.0-Linux	53.2	1065	Ga0255841	Gp0294137

Supplementary Table 4: qPCR assays used in the study

Assay	BML genera targeted (see Supplementary Table 4)	primer pair (5' to 3')	Assay source	qPCR standard used
Universal	all methanotrophs	A189F (GGN GAC TGG GAC TTC TGG) mb661R (GGT AAR GAC GTT GCN CCG G)	Kolb *et al*., 2003	*pmoA* from *Methylococcus capsulatus* Bath, cloned into PJET 1.2 plasmid. Cured plasmid was quantified with a Qubit HS kit, and serially diluted from 1.5 x 10^2 to 1.5 x 10^8 copies ml^{-1}
Methylococcus-group (type 1X)	*Methyloparacoccus, Methylococcus*	A189F (GGN GAC TGG GAC TTC TGG) mc468R (GCS GTG AAC AGG TAG CTG CC)	Kolb *et al.,* 2003	*pmoA* from *Methylococcus capsulatus* Bath*,* cloned into PJET 1.2 plasmid. Cured plasmid was quantified with a Qubit HS kit, and serially diluted*,* over 6 orders of magnitude, from 2.8 x 10^3 to 2.8 x 10^8 copies μl^{-1}.

Methylobacter group (type 1a)	*Methylobacter, Methylovulum, Methyloprofundus, Methylosoma*	mbac189F (GGN GAC TGG GAT TTC TGG) mb601R (ACR TAG TGG TAA CCT TGY AA)	modified from Kolb *et al.*, 2003. The primer A189F was replaced with mbac189f (5'-GGNGACTGGGATTTCTGG-3') based on analysis of a database of aligned *pmoA* sequences that indicated a single mismatch to A189f in many of these strains (Khadka et al., 2018).	*pmoA* (Accession OK157433) from *Methylobacter psychrophilus* strain FCN1, cloned into PJET 1.2 plasmid. Cured plasmid was quantified with a Qubit HS kit, and serially diluted over 6 orders of magnitude, from 3.0 x 10^3 to 3.0 x 10^8 copies µl-1. The strain FCN1 (Accession OK135604) was isolated from BML water using procedures described by Dedysh and Dunfield (2014), using medium 10 (Saidi-Mehrabad *et al.*, 2013) and incubation at 8^{o}C. Its 16S rRNA gene sequence matches ASV8 in Supplementary Table 2.